Solar Wind

A. Zaslavsky

14 janvier 2026

Table des matières

1 Introduction

1.1 Fluid equations

Here we recall the equations describing the evolution of the moments $(n, \mathbf{u}, p, ...)$ of the velocity distribution function of a population of point particles of mass m in a force field $\mathbf{F}$. The equations are presented here in the form that will be used in the rest of the course :

— Continuity equation (conservation of particle number), which relates the density n (scalar) to the average velocity $\mathbf{u}$ (vector) :

$$\frac{\partial n}{\partial t} + \text{div } n\mathbf{u} = 0 \tag{1}$$

— Momentum conservation equation, which relates the average velocity $\mathbf{u}$ (vector) to the pressure p (in the general case a second-order tensor ; in this course, to avoid overcomplicating matters, we will consider isotropic media, and therefore a scalar pressure $p = nkT$). Here we will consider a plasma in the totally non-collisional approximation, so we will neglect friction effects.

$$mn\left(\frac{\partial u}{\partial t} + \mathbf{u}\cdot\nabla\mathbf{u}\right) = -\nabla p + n\mathbf{F} \tag{2}$$

— Energy conservation equation, which relates internal energy (or pressure) to heat flux $\mathbf{j}_{th}$,

$$\frac{\partial}{\partial t}\left(nm\frac{u^2}{2} + \frac{3}{2}p\right) + \text{div}\left[\mathbf{u}\left(nm\frac{u^2}{2} + \frac{5}{2}p\right) + \mathbf{j}_{th}\right] = n\mathbf{u}\cdot\mathbf{F} + Q \tag{3}$$

In this equation, the term $\mathbf{j}_{th}$ describes heat transport by thermal conduction,

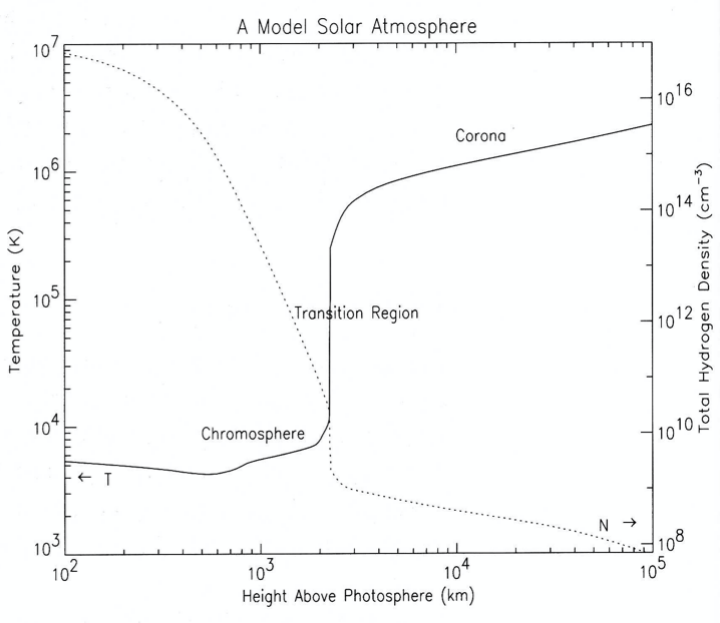

FIGURE 1 – Radial evolution of temperature and density between the chromosphere and the corona (numerical model).

while Q (in [W.m^{-3}]) describes heat transfer from a source outside the particle population under consideration ($Q > 0$ if heat enters the system).

— And an infinite series of equations relating to the additional moments of the distribution function. Since this infinite series cannot be solved, the system must be closed using a relation known as a *closure*, which links the highest-order moment to the lower-order ones. We will discuss below the closure relations that can be used in different cases.

The derivation of these equations from the kinetic equation describing the evolution of the distribution function of the particles in the population under consideration is presented in Appendix A.

2 Heating of the solar corona

2.1 The transition region

The solar corona, i.e. the upper region of the solar atmosphere, is separated from the chromosphere by a very thin boundary ($\Delta h \sim 100$ km), called the transition region. This boundary is characterised by a drastic change in temperature, over almost two orders of magnitude (see fig.1). We are interested here in describing this phenomenon, which is

important in the study of solar wind since, as we shall see in the next section, it is the thermal energy of the corona that is the source of the wind's acceleration.

2.2 Thermal instability

We consider the plasma present in the lower solar atmosphere, in the chromosphere and lower corona. In steady state ($\partial_t = 0$) and neglecting convection effects ($\mathbf{u} = 0$), the energy conservation equation (3) for this plasma takes the following form

$$Q = \text{div } \mathbf{j}_{th}, \tag{4}$$

which describes the steady state resulting from spatial redistribution, through thermal conduction of the heat locally injected per unit time Q. In the case of the solar atmosphere, the term Q has two dominant components : $Q = Q_c - Q_{ray}$. On the one hand, there is a heating term $Q_c > 0$, whose origin we do not know (see discussion below) but whose effects we can observe and are seeking to quantify. On the other hand, there is a radiative cooling term

$$Q_{ray} \simeq n_e n_H \Lambda(T) \tag{5}$$

The term Q_{ray} describes the loss of internal energy through radiation emission following the collisional excitation of ions present in the medium by electrons, hence its proportionality to the product $n_e n_H$. Assumptions are made about the abundance of ionic species per hydrogen atom and the probabilities of excitation, all of which are functions of temperature, which are taken into account in the factor $\Lambda(T)$. There is no simple expression for $\Lambda(T)$, but there are different models, one of which is illustrated in Fig.2. The important point is not so much the precise function as the fact that these functions have a maximum (around $\sim 10^5$ K). Above a certain temperature, cooling becomes less effective, resulting in a runaway effect. This is the physical reason for the existence of the transition region.

To evaluate the conduction term, we consider a Fourier-type law

$$\mathbf{j}_{th} = -\kappa \nabla T \tag{6}$$

where we use the Spitzer-Braginskii (SB) expression for κ,

$$\kappa = K_0 T^{5/2}, \qquad \text{with } K_0 \simeq 5.6 \times 10^{-12} \text{ W.m}^{-1}\text{K}^{-7/2} \tag{7}$$

valid in a fully ionised plasma (collisions are small-angle Coulomb deflections). It should be noted that the use of this expression for thermal conduction is controversial (see below) because it is not clear that the mean free path of the particles is sufficiently small compared to the gradient scales for it to be perfectly valid.

An order of magnitude assessment shows that

$$\frac{\text{div } \mathbf{j}_{th}}{Q_{ray}} \sim \frac{K_0 T^{7/2} L^{-2}}{n_e^2 \Lambda(T)} \ll 1 \tag{8}$$

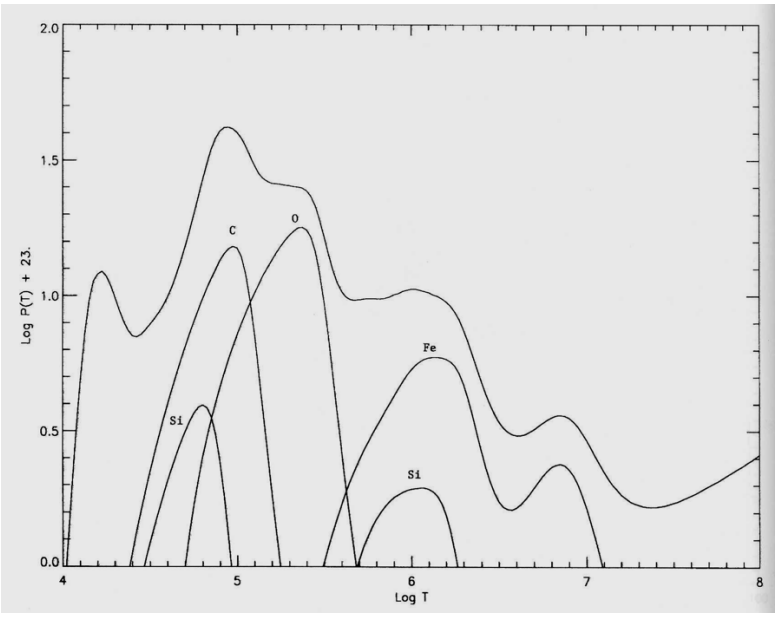

FIGURE 2 – Abscissa : log of temperature in K. Ordinate : log of the radiative cooling function $\Lambda(T)$ (here denoted P) in the solar corona, in erg.cm^3.s^{-1}. Reminder : 1 erg = 10^{-7} J. Therefore, multiply by a factor of 10^{-13} to convert to SI units [W.m^3.s^{-1}]. The emissions of different atomic lines used to calculate Λ are shown.

for typical conditions in the chromosphere (see fig.1), which is a "dense" and "cold" environment in which radiative transfer dominates. At the base of the transition region, the temperature is therefore determined by an equilibrium between the energy injection term and the radiative cooling term : $Q_c \simeq Q_{ray}$, and the local temperature is obtained by inverting the function Λ,

$$\Lambda(T) \simeq \frac{Q_c}{n_e^2} \tag{9}$$

However, the atmosphere near the solar surface is (approximately) exponentially stratified by gravity, $n_e \simeq n_0 \exp(-z/H)$ where z is the altitude and $H \sim kT/mg$ is the height scale : the higher you go, the fewer particles are capable of radiating energy. When the term Q_c/n_e^2 becomes greater than $\Lambda_{max} \sim 10^{-35}$ W.m^3.s^{-1}, the plasma is no longer dense enough to radiate the injected energy Q_c : the temperature rises sharply.

It is interesting to note that this phenomenon is largely independent of the amount of energy Q_c injected. Once a finite amount of energy is injected, given the exponential nature of density stratification, there will be an altitude at which thermal instability will develop. The critical density at which instability occurs can be easily calculated :

$$n_e \simeq \left(\frac{Q_c}{\Lambda_{max}}\right)^{1/2} \sim \left(\frac{Q_c}{1 \text{ W.m}^{-3}}\right)^{1/2} 10^{17} \text{ m}^{-3} \tag{10}$$

We can see that a heating rate of around $1 W.m^{-3}$ is consistent with observations.

2.3 Stabilisation by conduction

The temperature therefore increases in the transition region and only stabilises at a level where thermal conduction (which increases by $T^{5/2}$) becomes sufficient to stabilise the temperature gradient. We can return to the order of magnitude assessment (8) and see that, following the increase in temperature and decrease in density, we find ourselves just above the transition region, under the conditions of a dilute, hot plasma ($n \sim 10^{12}$ m^{-3} and $T \sim 10^6$ K), for which div $\mathbf{j}_{th} > Q_{ray}$. We can obtain an order of magnitude for the coronal temperature by completely neglecting radiative cooling,

$$T_{corona} \simeq \left(\frac{L^2}{K_0} Q\right)^{2/7} \sim \left(\frac{Q_c}{1 \text{ W.m}^{-3}}\right)^{2/7} 10^6 \text{ K} \tag{11}$$

where we have taken L to be the extremely short gradient scale of the transition zone $L \sim 100$ km. Here again, $Q_c \sim 1$ W.m^{-3} is consistent with the measured temperatures. Furthermore, the low exponent 2/7 means that the coronal temperature is not very sensitive to the exact value of Q, with a factor of 100 difference in Q_c producing only a factor of ~ 3 in T_{corona}. The model is simplistic, but it allows us to obtain the correct orders of magnitude.

2.4 Where does the energy come from ?

The obvious question is : what does Q_c represent ? We see that this term must exist, as the thermal instability of the transition region is its visible manifestation. The energy balance on a more global scale of the corona also shows that Q_c must be non-zero above the transition region. But we still need to identify the physical effect that causes this heat deposition in the plasma, and the source of the energy. This constitutes the "solar corona heating problem". It is one of the open problems in solar physics. A large number of models have been proposed, which can be classified into two main categories :

— Wave dissipation (AC models) : the idea is that acoustic or magneto-acoustic waves are excited by convective motions at the solar surface. These waves increase in amplitude with altitude and break into shock waves in which they can effectively transfer part of their energy to the plasma.

— Magnetic reconnection (DC models) : the idea is that the feet of magnetic flux tubes caught in the very dense plasma of the photosphere undergo random movements linked, again, to convective motions beneath the solar surface. The flux tubes at higher altitudes will therefore become entangled, twisted, generating strong current layers and Joule heating.

In all cases, the energy reservoir is found in the convective motions beneath the solar surface. All research on the subject consists of understanding how and through which channel this mechanical energy can be transported and degraded into thermal energy in the corona.

2.5 Collisionality, Knudsen number

The model described above gives a central role to the phenomenon of thermal conduction, which we described in the Spitzer-Braginskii approximation. This is well justified if the number of Coulomb collisions undergone by an electron on the typical temperature gradient scale is large :

$$K_n = \frac{\ell_{mfp}}{L} \ll 1 \tag{12}$$

where K_n is the Knudsen number. Let us try to estimate K_n for the typical parameters of the solar lower atmosphere. The mean free path of a particle with velocity v is $\ell_{mfp} = v/\nu_c$, where the Coulomb collision frequency is given by

$$\nu_c(v) = \frac{4\pi n_e e^4 \ln \Lambda_c}{(4\pi\varepsilon_0)^2 m_e^2 v^3} \tag{13}$$

$\ln \Lambda_c$ is here the Coulomb logarithm $\ln \Lambda_c \simeq \ln(12\pi n_e \lambda_d^3) \sim 20$ for the conditions of the transition zone and the corona. For a Maxwellian velocity distribution, we obtain

$$\ell_{mfp} = 8.9 \times 10^7 \frac{T_e^2}{n_e} \frac{17}{\ln \Lambda_c} \text{ m}, \tag{14}$$

whose application gives, in the chromosphere, $\ell_{mfp} \sim 3$ mm, which is obviously very small compared to all the scales involved. In the corona : $\ell_{mfp} \sim 10^8$ m, or $\sim 0.1 R_s$ where R_s is the solar radius : we are here in a weakly collisional environment. In the transition region (TR), taking the intermediate values of density and temperature, we obtain $\ell_{mfp} \sim 1$ km, which must be compared to the typical gradient scale, itself very small, to obtain the Knudsen number of the TR.

$$K_{n,RT} = \frac{\ell_{mfp}}{L} \sim 10^{-2}. \tag{15}$$

This number raises the question of the validity of the conduction coefficient κ. There is debate on the subject, but approaches (particularly numerical ones) seem to show that $K_n < 10^{-3}$ is a necessary condition for the validity of the SB approximation. The reason for the invalidity of the approximation lies largely in the dependence of ν_c (13) on v : regardless of the velocity distribution (if it is not on a bounded support), there will be particles that behave in a non-collisional manner. Indeed, the Knudsen number depends strongly on the velocity of the particle in question :

$$K_n(v) \simeq \frac{v}{\nu_c(v) L} \simeq \frac{(4\pi\varepsilon_0)^2 m_e^2}{4\pi e^4 \ln \Lambda_c} \frac{v^4}{n_e L} \simeq 6.2 \times 10^{-8} \frac{v^4}{n_e L} \tag{16}$$

This can be estimated by introducing the thermal velocity of electrons $v_{th} = \sqrt{kT/m_e}$, and for typical parameters of the transition zone,

$$K_n(v) \sim 10^{-2} \left(\frac{v}{v_{th}} \right)^4 \tag{17}$$

2.6 Ballistic model : gravitational velocity filtering

The non-collisionality of the most energetic particles can have unexpected effects, and in particular create temperature inversions with altitude without any external energy or heat input (given the particle distributions at the base of the transition region).

Let us assume a Maxwellian particle distribution at $z = 0$. The distribution function (reduced, i.e. integrated over the two directions perpendicular to the z axis taken vertically) at higher altitudes is given by

$$f_M(v) = \frac{n_0}{\sqrt{2\pi kT/m}} \exp\left(-\frac{mv^2}{2kT} \right) \exp\left(-\frac{mgz}{kT} \right). \tag{18}$$

The terms depending on position and velocity are separated, and the temperature is therefore independent of altitude. We therefore have an isothermal atmosphere, whose density changes exponentially with altitude according to the law

$$n(z) = n_0 \exp -\frac{z}{H}. \tag{19}$$

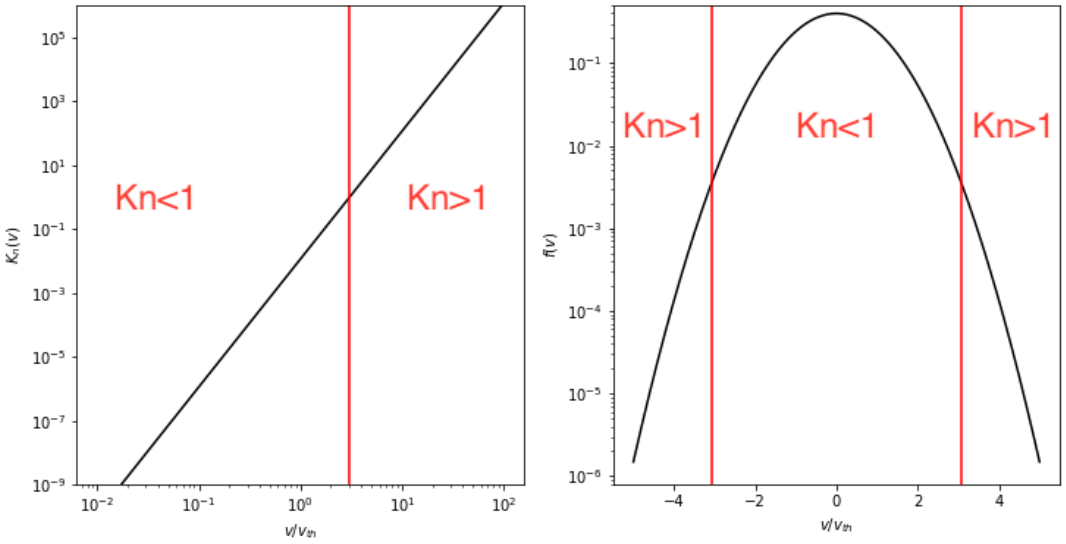

FIGURE 3 – Knudsen number as a function of v/v_{th} (left) and Maxwellian distribution function with "collisionality" limits. We can see that particles above three thermal velocities no longer undergo collisions over the extent of the RT.

where the height scale is given by $H = kT/mg$.

Now let us assume a 'non-thermal' distribution function at the base of the transition region, characterised by an excess of high-energy particles compared to the Maxwellian distribution. A very simple model of such a distribution is a sum of two Maxwellian distributions, one with temperature T_c and density n_c, and the other with temperature $T_h \gg T$ and density $n_h \ll n$. The total density is $n = n_c(z) + n_h(z)$ and the total temperature is defined by the variance of the particle velocities

$$T = \frac{m < v^2 >}{k} = \frac{n_c T_c + n_h T_h}{n_c + n_h} \tag{20}$$

In a model without any collisions, where the particles follow ballistic trajectories in the solar gravitational field, the evolution of the densities of each of the two particle populations is given by (19), where each population is characterised by a different height scale. The temperature (more precisely, here, the variance of velocities) therefore evolves with altitude

$$T(z) = \frac{n_{c0} T_c \exp(-z/H_c) + n_{h0} T_h \exp(-z/H_h)}{n_{c0} \exp(-z/H_c) + n_{h0} \exp(-z/H_h)} \tag{21}$$

Figure 4 shows an example of the evolution of temperature and density for a distribution function with non-thermal tails. We observe a characteristic of the velocity filtering effect : densities and temperatures are anti-correlated (which corresponds to a polytropic index less than 1). This is easy to understand : the most energetic particles

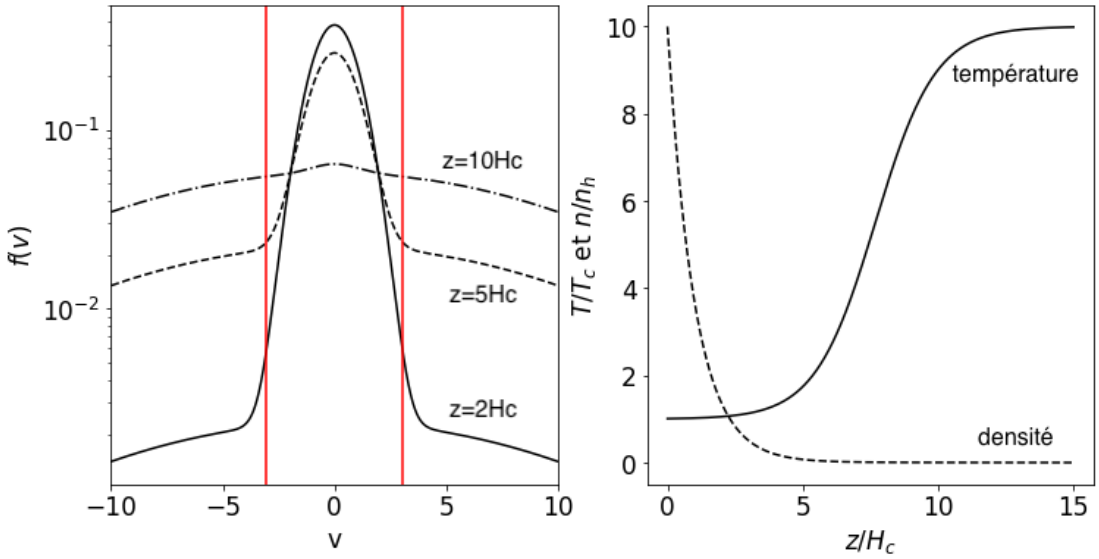

FIGURE 4 – Distribution function with non-thermal tails (left) and evolution of density and temperature with altitude (right).

rise higher. Thus, beyond a few height scales of the lower temperature population, only the most energetic particles remain, which are also the least collisional. The less energetic particles have been "filtered out".

The model presented in this section is simplified in that it only takes into account the gravitational potential in which the particles evolve. A more complete model would also take into account a more complex potential, but the fundamental idea is the one illustrated here. It can be shown that when the potential is attractive, the temperature increases, whereas when it is repulsive, the temperature decreases.

We can see that velocity filtering makes it possible to reproduce the sudden temperature jump in the transition zone. However, it leaves open the question of the formation of the suprathermal population and its maintenance in an environment as collision-prone as the chromosphere. This poses the heating problem in a slightly different way : heating is still necessary, but the challenge now is to find a process capable of preferentially injecting energy into high-energy particles. Wave-particle interaction mechanisms, for example.

2.7 Bibliography

Corona heating :

— Dynamics of the Quiescent Solar Corona, R. Rosner, W.H. Tucker and G.S. Vaiana, The Astrophysical Journal, 220 :643-665, 1978.

— The Properties of the Solar Corona and Its Connection to the Solar Wind, S.R. Cranmer and A.R. Winebarger, Ann. Rev. Astron. Astrophys. 57, 2019.

Thermal transport in plasmas :

— Transport Phenomena in a Completely Ionised Gas, Spitzer L. and R. Härm, Phys Rev, 89, 1953.

— Transport processes in a plasma, Braginskii, S. I., Reviews of plasma physics 1 : 205, 1965

Gravitational filtering :

— On the Causes of Temperature Change in Inhomogeneous Low-Density Astrophysical Plasmas, J.D. Scudder, Astrophysical Journal v.398, p.299, 1992 Why All Stars Should Possess Circumstellar Temperature Inversions, J.D. Scudder, Astrophysical Journal v.398, p.319, 1992

3 The solar wind

In this section, we examine one consequence of the existence of a very high-temperature corona : the evaporation of this corona into the interplanetary medium in the form of a supersonic expanding plasma wind, the solar wind.

3.1 The problem of a static corona

Here we consider the possibility of maintaining a static solar atmosphere at high altitudes. The equation describing the plasma is (see eq.(2))

$$\frac{dp}{dr} = -n\frac{mMG}{r^2} = -p\frac{mMG}{kTr^2} \tag{22}$$

from which we derive the pressure as a function of distance r from the center of the Sun,

$$p(r) = p(r_0)\exp\left(-\frac{mMG}{k}\int_{r_0}^{r}\frac{dr}{T(r)r^2}\right), \tag{23}$$

which expresses the relationship between pressure and temperature profiles in a gravitational field. In particular, we see that in order to have zero pressure at infinity (i.e., an atmosphere entirely confined by gravity), the temperature must decrease faster than $T(r) \sim r^{-1}$. In a medium as thermally conductive as a fully ionised plasma, such a steep profile is unlikely.

The profile $T(r)$ can be estimated (at least in order of magnitude) by assuming that it is essentially determined by thermal conductivity. We can use eq.(3) in steady state,

$$\mathrm{div}\,(-\kappa(T)\nabla T) = Q \tag{24}$$

which, integrated over a volume between two spheres of radius r_0 and r, assuming spherical symmetry, gives

$$-4\pi r^2\kappa(T)\frac{dT}{dr} + 4\pi r_0^2\kappa(T_0)\left.\frac{dT}{dr}\right|_{r0} = \int_{r_0}^{r} Q(r)4\pi r^2 dr \tag{25}$$

or, more compactly

$$\Phi(r) - \Phi(r_0) = P(r, r_0) \tag{26}$$

where $\Phi(r)$ is the power transported by conduction through a sphere of radius r, and $P(r, r_0)$ is the power deposited locally via the term Q between radius r_0 and radius r. The temperature profile can be obtained by imposing a boundary condition $r \to \infty$ (we take $T(r \to \infty) = 0$), by making explicit the conductivity $\kappa(T)$ (we take the SB expression eq.(7), $\kappa = K_0 T^{5/2}$). We obtain

$$T^{7/2}(r) = \frac{7\Phi_0}{8\pi K_0 r} + \int_r^{\infty} \frac{7P(r, r_0)}{8\pi K_0 r^2} dr. \tag{27}$$

This equation allows us to discuss the temperature profile : by neglecting the local term, we see that thermal conduction to the outside induces a profile of $T(r) \propto r^{-2/7}$, which therefore decreases much less rapidly than $T(r) \propto r^{-1}$ required for gravitational confinement of the corona according to eq.(23). An estimate of the power term shows that it will necessarily be negligible compared to Φ_0 after a certain distance.

These arguments show us that the confinement of the atmosphere by solar gravity alone is therefore impossible : a static atmosphere will necessarily have a non-zero pressure p_∞ at infinity, and static equilibrium can only be ensured through the existence of a "confining" medium with at least this pressure. The medium in question could be the interstellar medium. Its pressure is $p_{is} \simeq 10^{-14}$ Pa. Let us calculate the pressure at infinity for a temperature profile of the form $T = T_0(r/r_0)^{-\alpha}$ (where $\alpha = 2/7$ in the hypothesis of the profile provided by SB conduction). Calculating the integral (23) gives

$$p_\infty = p(r_0)\exp\left(-\frac{mMG}{kT_0}\frac{1}{r_0(1-\alpha)}\right) \approx p(r_0)\exp\left(-\frac{10^7\ \mathrm{K}}{T_0(1-\alpha)}\right), \tag{28}$$

which allows us to express the condition of a static atmosphere in the form of a condition on the temperature on the corona. Noting that the pressure at the base of the corona is of the order of $p(r_0) = 2nkT_0 \sim 3 \times 10^{-5}$ Pa, we obtain

$$(1-\alpha)T_{stat} \sim \frac{10^7}{\ln(p(r_0)/p_{is})} \sim 5 \times 10^5\ \mathrm{K} \tag{29}$$

Thus, the high temperature of the corona, due to the thermal instability of the transition region, combined with the high thermal conductivity of the plasma, makes it impossible for the atmosphere to be confined by the interstellar medium.

It should be noted that the impossibility of confinement is not due solely to the high coronal temperature. In fact, an atmosphere at several million Kelvin could be confined if the temperature gradient were slightly higher than it is, i.e. if thermal conduction were slightly less efficient. For example, according to (29), a corona at 1 MK would be confined with an index $\alpha \simeq 3/5$.

3.2 Parker model

If the atmosphere cannot be static, then it must be dynamic (yes, indeed). Let us therefore study a model that models the coronal plasma without neglecting its average velocity $\mathbf{u}$. Such a model (as well as the observation that static confinement is impossible) was developed in 1958 by Eugene N. Parker (i.e. one year before the launch of the first space probe to measure solar wind plasma). Here we describe the model that bears his name.

We consider a plasma consisting of electrons and protons. Assuming the system to be spherically symmetric, with the sun at the center, we will consider that the physical quantities depend only on the coordinate r. We also consider that the velocity field is purely radial, $\mathbf{u} = u\mathbf{e}_r$. In steady state, the equations of evolution of the densities and radial components of the average electron and ion velocities are given by the fluid equations (1) and (2) :

$$\frac{d}{dr}\left(r^2 n_e u_e\right) = 0, \qquad \frac{d}{dr}\left(r^2 n_p u_p\right) = 0 \tag{30}$$

and

$$n_e m_e u_e \frac{d}{dr} u_e = -\frac{dp_e}{dr} - e n_e E - n_e m_e \frac{GM}{r^2} \tag{31}$$

$$n_p m_p u_p \frac{d}{dr} u_p = -\frac{dp_p}{dr} + e n_p E - n_p m_p \frac{GM}{r^2} \tag{32}$$

Here we have neglected the effects of a possible radial component of the Laplace force $\mathbf{j} \times \mathbf{B}$. This can be justified by considering that the magnetic field lines are also radial.

Assuming that the charge density $\rho = e(n_p - n_e)$ is close to zero everywhere (assumption of plasma electro-neutrality), and that the radial component of the current density $j_r = e n_p u_p - e n_e u_e$ is also zero everywhere (the Sun does not charge), we have :

$$n_e \simeq n_p \simeq n \qquad \text{and} \qquad u_e \simeq u_p \simeq u. \tag{33}$$

By adding the momentum evolution equations and neglecting m_e compared to m_p, we obtain the evolution equation for u :

$$n m_p u \frac{d}{dr} u = -\frac{d}{dr}\left(nk(T_e + T_p)\right) - n m_p \frac{GM}{r^2} \tag{34}$$

To continue, we need a *closure* for the fluid equations, i.e. a relation linking the highest-order fluid momentum (here the pressure p) to the lower-order momenta. Following Parker's first article on the subject, we choose the simplest one and consider that the electron and ion temperatures are independent of r (isothermal expansion) in the wind acceleration region, i.e. between the transition zone and a few solar radii. This assumption is justified by the high thermal conductivity of plasma, which, as we have seen, greatly reduces the temperature gradient.

We can then set (34), using the continuity equation to eliminate the density n, in the form :

$$\left(u^2 - c_s^2\right) \frac{1}{u} \frac{d}{dr} u = \frac{2c_s^2}{r} \left(1 - \frac{r_c}{r}\right) \tag{35}$$

where we have introduced the speed of sound $c_s^2 = k(T_e + T_p)/m_p$ and the critical radius $r_c = GM/2c_s^2$.

This equation can be integrated by separation of variables :

$$\frac{u^2}{2} - c_s^2 \ln u = 2c_s^2 \ln r + 2c_s^2 \frac{r_c}{r} + C \tag{36}$$

where C is the integration constant. The value of C determines the behaviour of the solution. There are two families of solutions (see fig.5) : (i) supersonic solutions, satisfying $u > c_s$ for all r and whose velocity profile has a minimum at $r = r_c$. These solutions already have very high velocities in the transition zone and are therefore not of interest for the expansion problem we are trying to address. (ii) subsonic solutions, satisfying $u < c_s$ for all r and whose velocity profile passes through a maximum at $r = r_c$. We see from eq.(35) that for these solutions, $u \sim r^{-2}$ when $r \to \infty$. According to the continuity equation, we therefore have $n \sim 1/(r^2 u) = cste$ when $r \to \infty$. These solutions are therefore characterised by a non-zero density and pressure at infinity, and by the need for a confining medium. However, they are not physically excluded, and there was a debate about whether they were physically achievable before the first space measurements were taken.

The latter showed that the realised solution was precisely the "limit" solution, which Parker had intuited, between the two aforementioned families : the transonic solution, with low speed near the Sun and supersonic speed at large distances, for which we have $u(r_c) = c_s$, which is a condition for the derivative of u not to be zero at $r = r_c$.

The condition $u(r_c) = c_s$ allows us to determine the value of the constant C for the transonic case. We obtain $C = -c_s^2(3/2 + \ln c_s + 2\ln r_c)$, and equation (36) takes the dimensionless form

$$\frac{u^2}{2c_s^2} - \ln \frac{u}{c_s} = \ln \left(\frac{r}{r_c}\right)^2 + \frac{2r_c}{r} - \frac{3}{2}, \tag{37}$$

which can be used to study the asymptotic behaviour of the solution. In particular, we see that for $r \gg r_c$, $u \sim 2c_s\sqrt{\ln(r/r_c)}$: for energy reasons, isothermal expansion cannot

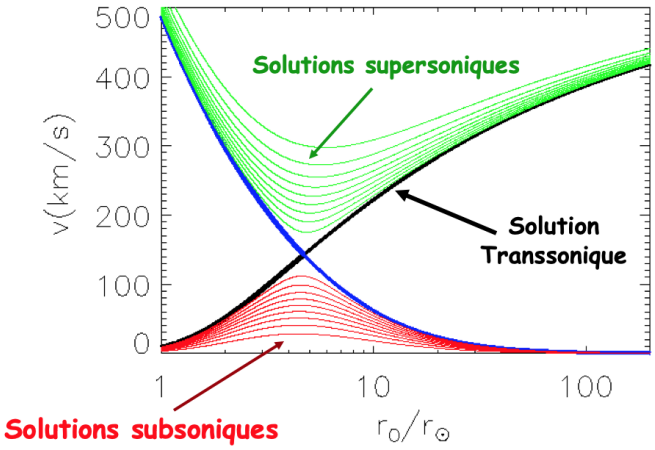

FIGURE 5 – Different families of solutions illustrated in the (u,r) plane

be maintained very far from the Sun.

Assuming that the electron and ion temperatures are equal just above the TR, we have the following estimate of the critical radius ($R_s \simeq 7 \times 10^8$ m is the solar radius),

$$r_c \simeq \frac{GMm_p}{4kT} \simeq 5.8 \left(\frac{10^6 \text{ K}}{T}\right) R_s \tag{38}$$

We can therefore see that the higher the temperature at the TR outlet, the closer the critical radius will be to the Sun. In practice, the coronal temperature is of the order of a million degrees and $r_c \sim 5R_s$: the thermal conductivity must therefore maintain a low temperature gradient over a few solar radii to justify the isothermal hypothesis. It should be noted that this hypothesis is not crucial to the existence of the wind. A calculation similar to the one performed in this section can be carried out for the more general case of a polytropic closure equation of the type $d(pn^{-\gamma}) = 0$, where γ is the polytropic index (equal to 1 for the isothermal case, equal to 5/3 for the adiabatic case).

For an initial estimate of the wind speed at the exit of the acceleration zone, we can use the estimate $u \sim 2c_s\sqrt{\ln(r/r_0)}$. Since the root of the logarithm varies very slowly for large arguments, we can take, for example, at 10 R_s, $\sqrt{\ln(10)} \sim 1.5$, or

$$u_\infty \simeq 3 \left(\frac{2kT}{m_p}\right)^{1/2} \simeq 385 \left(\frac{T}{10^6 \text{ K}}\right)^{1/2} \text{ km.s}^{-1} \tag{39}$$

This model reproduces the observed velocities in order of magnitude, particularly in the slow wind. However, it does not solve the problem of the fast wind, which originates from coronal holes (characterised by open magnetic field lines) and is measured at nearly 800 km.s^{-1}. To explain such accelerations, a coronal temperature of $T \sim 5$ MK would be

required, which is far from being observed (especially since coronal holes are generally colder regions than the rest of the corona).

3.3 Mass flux

We can use Parker's model to derive a particularly interesting characteristic quantity, which is the mass flux of the solar wind : what fraction of the star's mass evaporates per unit of time ? The mass flux $\dot{M} = 4\pi r^2 n m_p u = cste$ according to the continuity equation.

Equation (37) gives us $\dot{M}$, allowing us to estimate the wind speed in the lower layers of the corona, which we know to be very small compared to c_s. We can therefore neglect the term in u^2/c_s^2 compared to the term in log. We obtain

$$u(r \to 0) \simeq c_s \left(\frac{r_c}{r}\right)^2 \exp\left(-\frac{2r_c}{r} + \frac{3}{2}\right) \tag{40}$$

and therefore

$$\dot{M} \simeq 4\pi n_0 m_p c_s r_c^2 \exp\left(-\frac{2r_c}{R_s} + \frac{3}{2}\right) \tag{41}$$

where we have neglected the distance between the solar surface and the top of the transition region. The expression for r_c (eq.38) allows us to estimate the mass flux as a function of the corona temperature,

$$\dot{M} \sim 10^{13} \left(\frac{T}{10^6 \text{ K}}\right)^{-3/2} \exp\left(-\frac{11.10^6 \text{ K}}{T}\right) \text{kg.s}^{-1} \tag{42}$$

On the one hand, we can comment on the order of magnitude $\dot{M} \sim 10^8$ kg.s^{-1}, which, although impressive, remains quite low compared to solar scales. The solar mass is $M \sim 10^{30}$ kg, the timescale over which this evaporation would have a significant effect is $\tau_M = M/\dot{M} \sim 240000$ billion years, whereas the estimated age of the solar system is 5 billion years.

On the other hand, we can note the extreme sensitivity of this mass flux, via the exponential factor, to the temperature of the corona, illustrated in Figure 6. If the solar atmosphere were at the photospheric temperature of approximately 6000 K, the mass flux would be divided by a factor of $\sim 10^{430}$. This clearly shows the decisive importance of the instability of the transition region in the existence of a solar wind.

3.4 Polytropic closures, conditions for the existence of the solar wind.

The solar wind flow described by (34) is potential (all viscosity terms have been neglected). This translates into the existence of an integral for this equation, which can

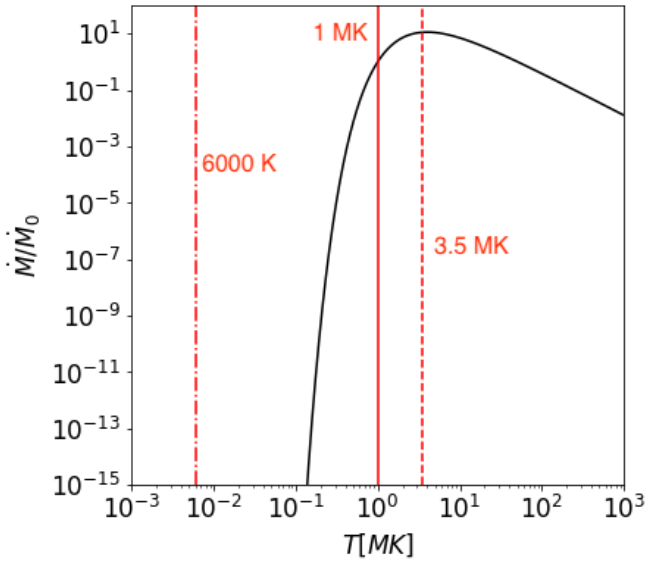

FIGURE 6 – Mass flux as a function of coronal temperature. The temperature at which the maximum is reached is indicated by the dotted line. The temperature of the photosphere is shown for reference.

be calculated, for example, by evaluating the variation in mechanical energy of a particle under the effect of pressure forces :

$$\Delta_{1\to 2}\left(\frac{mu(r)^2}{2}-\frac{Gm_pM}{r}\right)=-\int_{r_1}^{r_2}\frac{1}{n}\frac{dp}{dr}dr=-\int_{p_1}^{p_2}\frac{dp}{n} \tag{43}$$

where $p = p_p + p_e$.

We can see that the right-hand side of this equation (the work done by the pressure forces) depends entirely on the choice of closure relation selected for the fluid equations. For the isothermal closure studied previously, we obtain the integral

$$\frac{u(r)^2}{2}+\frac{k(T_p+T_e)}{m}\ln(n)-\frac{GM}{r}=\mathscr{E} \tag{44}$$

Where $\mathscr{E}$ is energy per unit mass. We can express n in this equation using the continuity equation (introducing the particle flux $F = \dot{M}/4\pi m_p$)

$$\frac{u^2}{2}-c_s^2\ln u=2c_s^2\ln r-c_s^2\frac{2r_c}{r}+\mathscr{E}-\ln F \tag{45}$$

which is obviously identical to equation (36) where the integration constant $C \equiv \mathscr{E} - \ln F$. We have studied the properties of this equation in the previous sections. And we have

seen, among other things, that the isothermal hypothesis had the flaw of a speed diverging to infinity.

We can generalise the treatment somewhat by considering other closure relations. One possible choice is the empirical polytropic relations, linking pressure and density in the form

$$\frac{d}{dr}\left(pn^{-\alpha}\right) = 0, \tag{46}$$

where α is the polytropic index. We see that the choice of $\alpha = 1$ corresponds to an isothermal closure, while $\alpha = c_p/c_v = \gamma = 5/3$ corresponds to an adiabatic closure—that is, without heat input into the plasma (exercise : verify this using the energy conservation equation eq.3). Eq.(46) allows us to explicitly calculate the enthalpy term (right-hand side of eq.43), and obtain Bernoulli's equation :

$$\frac{u(r)^2}{2} + \frac{\alpha_e}{\alpha_e - 1}\frac{kT_e(r)}{m_p} + \frac{\alpha_p}{\alpha_p - 1}\frac{kT_p(r)}{m_p} - \frac{GM}{r} = \mathscr{E} \tag{47}$$

The specific energy $\mathscr{E}$ is determined by the boundary conditions at the base of the flux tube. Here, we have considered the possibility of different closure relations and temperature profiles for electron and proton fluids, since the low Knudsen number in the solar corona does not justify a priori collision coupling of the two populations.

As in the isothermal case, the continuity equation allows us to express Eq. (47) in the form of an equation linking u to r, by expressing the enthalpy terms :

$$\frac{\alpha}{\alpha - 1}\frac{kT(r)}{m_p} = Au^{1-\alpha}r^{2-2\alpha}, \qquad \text{where } A = \frac{\alpha}{\alpha - 1}\frac{p_0 n_0^{-\alpha} F^{\alpha-1}}{m_p} \tag{48}$$

The properties of equation (47) with (48) have been extensively studied by Parker in the case where the electron and ion temperature profiles are identical ($T_e(r) = T_p(r)$, and therefore $\alpha_e = \alpha_p$). We will not reproduce this study in the context of this course, but we will note the following interesting result : a condition for the existence of a transonic wind is that $\alpha < 3/2$. Above this value, and therefore in particular for the case of interest of adiabatic expansion $\alpha = 5/3$, there is no critical solution. Once again, we see the importance of thermal conduction in the production of wind.

Equation (47) allows us to discuss the conditions for the existence of a solar wind. Indeed, if the indices $\alpha > 1$, we see that density and temperature are positively correlated. The decrease in density $n \sim r^{-2}$ will therefore be accompanied by a decrease in temperature $T \sim r^{-2(\alpha-1)}$. We can therefore assume that the enthalpy terms $\propto T(r)$ in (47) will be negligible compared to the kinetic energy term when $r \to \infty$. We then have

$$\mathscr{E} \simeq \frac{1}{2}mu_\infty^2 \simeq \frac{\alpha_p k T_{p0}}{\alpha_p - 1} + \frac{\alpha_e k T_{e0}}{\alpha_e - 1} - \frac{GMm}{R_s} \tag{49}$$

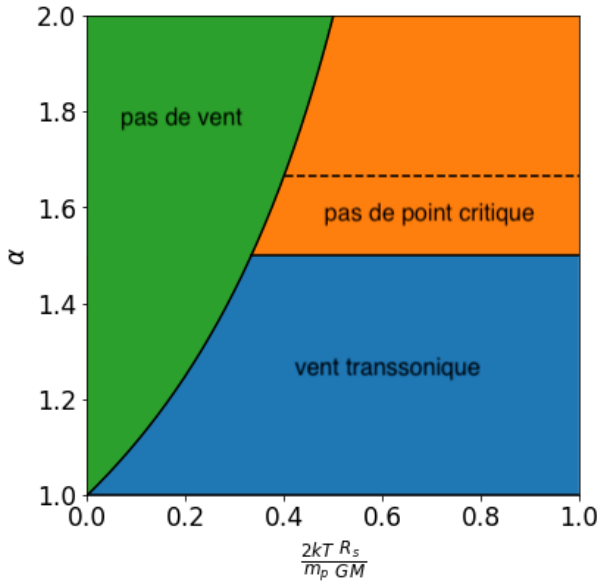

FIGURE 7 – Condition of existence for $T_e = T_p = T$. Thermal energy normalised by gravitational energy on the x-axis, polytropic index on the y-axis. The dotted line shows the adiabatic index $\gamma = c_p/c_v$.

where the condition $\mathscr{E} > 0$ is necessary (but not sufficient) for the existence of a solar wind. This expression describes the acceleration of the solar wind from an energy perspective : its terminal velocity is determined by the energy available to create pressure forces at the base of the flux tube. For a solar wind to exist, this energy must be sufficient to allow particles to escape from the solar gravitational potential well $-GMm/R_s$.

Figure 7 shows the possibilities of existence in a plane (x, α), where the dimensionless parameter on the x-axis is $x = \frac{2kT_0}{m_p}\frac{R_s}{GM} = \frac{R_s}{r_c} = \frac{4c_s^2}{v_{lib}{}^2}$. We can see that for an index $\alpha = 1$ corresponding to an isothermal evolution, we will obtain a supersonic wind regardless of the value of the parameter x, i.e. even in the case $x \to 0$ (however, as we saw in the section on mass flow, there will not necessarily be much matter in this wind). Isothermal expansion assumes the existence of a thermostat, which can provide unlimited energy to drive the pressure forces. For indices $\alpha > 1$, corresponding to finite energy injections into the plasma, a finite base temperature is also required for the wind to blow. For typical parameters in the transition zone, we have $x \sim 0.3$. We therefore have a maximum polytropic index $\alpha \sim 1.4$.

Finally, note that according to the form of eq.(49), if one of the populations is adiabatic (protons, for example) while the other is isothermal (or has a polytropic index $\alpha < 3/2$), the wind can exist. This may seem strange, since we have not specified a

coupling mechanism between the populations. We will see later that the electric field is responsible for this coupling. It does not appear explicitly in the equations, but acts through the constraint of electroneutrality.

3.5 Energy flux

When studying polytropic cases, we truncated the fluid equations at the second moment, linking pressure p to density n. This amounts to making an assumption about the higher-order equation, which describes energy conservation. Polytropic equations, while facilitating the analytical study of the problem, impose a strong constraint on the form of energy exchanges, which is difficult to justify physically.
To avoid this problem, we must take into account the energy conservation equation (as we did in the section describing the static corona, but this time without neglecting the velocity terms)

$$\text{div}\left[\mathbf{u}\left(nm_p\frac{u^2}{2}+\frac{5}{2}p\right)+\mathbf{j}_{th}\right]=-n\mathbf{u}\cdot\frac{GMm_p}{r^2}\mathbf{e}_r+Q \tag{50}$$

where we have assumed steady state and spherical symmetry. By integrating this equation between two spheres of radius r_0 and r, and introducing $\dot{M}=4\pi nm_p ur^2=cste$, we obtain

$$\dot{M}\left[\left(\frac{u^2}{2}+\frac{5}{2}\frac{kT_p}{m_p}+\frac{5}{2}\frac{kT_e}{m_p}-\frac{GM}{r}\right)\right]_{r_0}^{r}-\left[4\pi r^2\kappa(T)\frac{dT}{dr}\right]_{r_0}^{r}=\int_{r_0}^{r}Q(r)4\pi r^2dr \tag{51}$$

or more compactly,

$$\dot{M}\left(\mathscr{E}(r)-\mathscr{E}(r_0)\right)=-\Phi(r)+\Phi(r_0)+P(r,r_0) \tag{52}$$

where $\mathscr{E}$ is the energy per unit mass defined in the previous section by eq.(**??**), for an adiabatic index $\alpha_e=\alpha_p=\gamma=5/3$. $\dot{M}\mathscr{E}(r)$ is therefore the energy flux of the solar wind. $\Phi(r)$ is the heat flux through the sphere of radius r and $P(r,r_0)$ describes the local plasma power balance (same definitions as in the section on the static corona).

Equation (**??**) therefore links the solar wind energy flux to the source terms, which are the heat flux and the deposited energy. Neglecting the latter (pragmatically, we do not know its form), and neglecting the heat flux away from the Sun relative to its value in the corona $\Phi_0\equiv\Phi(r_0)$, we obtain for the solar wind energy flux for $r\to\infty$

$$\dot{M}\mathscr{E}(r)\simeq\dot{M}\mathscr{E}(r_0)+\Phi_0 \tag{53}$$

which can also be expressed by showing the velocity at infinity

$$u_\infty^2=2\mathscr{H}_0-u_{lib}^2+\frac{2}{\dot{M}}\Phi_0 \tag{54}$$

where we have introduced the escape velocity of the Sun $u_{lib}^2=2GM/R_S\simeq 618$ km.s^{-1}, and the mass enthalpy $\mathscr{H}_0=5k(T_{p0}+T_{e0})/2m_p$. The first term represents the thermal

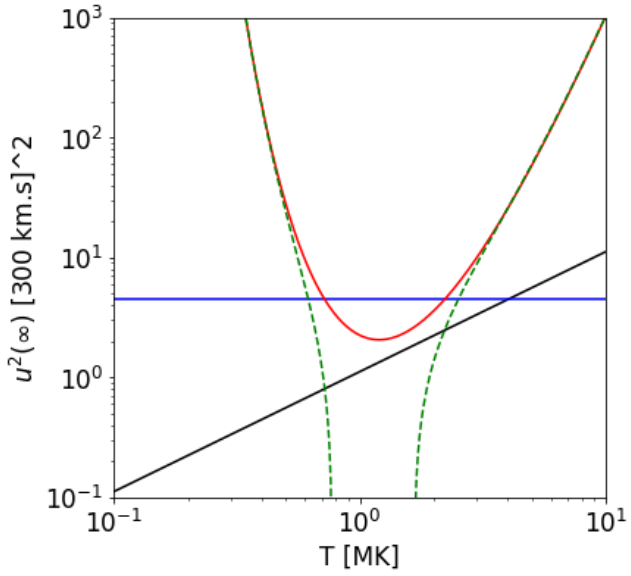

FIGURE 8 – The different terms in equation (54). Blue : gravitational potential. Red : heat flux. Black : enthalpy. Dotted lines : sum.

energy available at the base of the corona, the second the depth of the gravitational potential well to be overcome, and the third the energy injected by thermal conduction.

An evaluation of the terms in order of magnitude, using the SB conductivity, gives the following for coronal conditions : $\Phi_0 \sim 1.2 \times 10^{19}$ W, $\dot{M}\mathscr{H}_0 \simeq 0.5.10^{19}$ W and $\frac{1}{2}\dot{M}u_{lib}^2 \simeq 2.10^{19}$ W. We are "just" right in terms of energy to have a wind far from the Sun ($u_\infty^2 > 0$).

However, the orders of magnitude are correct. It is important to remember that $\dot{M}$, and therefore the energy flux, is extremely sensitive to the coronal temperature. It is instructive to plot the total energy flux as a function of the coronal temperature, using the expression for $\dot{M}(T)$ derived previously for the isothermal case. We find

$$u_\infty^2 \sim 10^{11}\left(\frac{T}{10^6\text{K}} - 4\right) + 5.10^8\left(\frac{T}{10^6\text{K}}\right)^5 \exp\frac{6.10^6\text{ K}}{T} \tag{55}$$

Figure 8 illustrates these different terms. We can see that in the observed operating range, around 1MK, the balance is negative : there is a lack of energy. An energy injection term Q is therefore certainly necessary for the existence of a wind. This is particularly critical for the fast wind - hypotheses are that it is accelerated by Alfvén waves and possible cyclotron heating of protons.

It should also be remembered that these estimates are made using assumptions (SB

conductivity, neglect of the magnetic field, equivalent electron and ion temperatures, etc.) that can be played with. But ultimately, the consensus is that there is a slight energy deficit to accelerate the wind.

Finally, although this goes beyond the scope of this course, it should be noted that a solar wind model can be constructed from fluid equations including the energy equation, with a closure on the heat current density $\mathbf{j}_{th}$. This work was done as early as 1960 by Chamberlain, taking the expression SB for $\mathbf{j}_{th}$ - however, he used the assumption of $u \to 0$ far from the Sun (he believed at the time that the solution achieved was subsonic). Today, most models are numerical and use more or less ad hoc relationships for $\mathbf{j}_{th}$, mixing transport effects and ballistic effects as a function of density, temperature and the local magnetic field (which is conspicuously absent from this section).

3.6 The role of the electric field

In the sections on polytropic expansion and energy balance, we noted that the enthalpy terms involved the sum of the electron and ion pressures. One consequence of this is that a wind could exist even if one of the populations did not meet the conditions for existence, as long as the other compensated for it. The two populations therefore do not behave independently, even though no explicit coupling term (e.g. collision) between the populations has been introduced.

The model used does not explicitly involve the electric field. However, the electric field obviously plays a role in that it guarantees electro-neutrality. To intuitively understand the role of the electric field as a "transmission belt" between ions and electrons in the dynamics of electrons and ions, let us study the following simplified model.

First, we neglect the mass of electrons : $m_e \to 0$. According to (31), electrons are therefore in a state of hydrostatic equilibrium :

$$\frac{dp_e}{dr} = -en_eE \tag{56}$$

Now let us assume that the temperature of the protons is negligible : $T_p \to 0$. Under this assumption, "alone" protons (or a neutral gas) would obviously be confined by the solar atmosphere. The equation describing the evolution of the protons' velocity is written as

$$n_pm_pu_p\frac{d}{dr}u_p = en_pE - n_pm_p\frac{GM}{r^2} = -\frac{dp_e}{dr} - n_pm_p\frac{GM}{r^2}. \tag{57}$$

This equation has been solved previously and, in this case, obviously depends only on the closing relation of the electrons. This can be interpreted as follows : the (hot) electrons drive the (cold) protons against the effect of gravity by producing an electric field E, whose action forces electrons and protons to move together. The previous equation allows us to express this electric field as

$$E = \frac{-1}{en_e}\frac{dp_e}{dr} = \frac{m_p}{e}\left(\frac{GM}{r^2} + u_p\frac{du_p}{dr}\right) \tag{58}$$

The first term is present even in a static atmosphere. This is the so-called "Panekoek-Rossland" field, which plays an important role in ionised static atmospheres (we will see this in the course on the Earth's ionosphere). The second term depends on the proton velocity profile, which is itself determined by the form of the electron pressure term p_e, and therefore by the form of the electron closure equation. This simple model gives an insight into how the interplanetary electric field and the electron closure equation are closely related.

3.7 Bibliography

— Interplanetary Dynamical Processes, Eugene Newman Parker, Interscience Publishers, New York, 1963
— Dynamics of the Interplanetary Gas and Magnetic Fields, Eugene N. Parker, Astrophysical Journal, vol. 128, p.664, 1958
— Stellar Winds Mechanisms and Instabilities, S. Owocki, Evolution of Massive Stars, Mass Loss and Winds, EAS Publication Series, 13, 2004

4 The Interplanetary Magnetic Field

We know that the Sun is magnetised. At the lowest order, its field is dipolar, but close to its surface it is much more structured and complex. This structure obviously has effects on the structure of the solar wind itself and on its acceleration. The model developed in the previous section, in spherical symmetry, is not modified by the presence of a radial field, so we can assume (and this is why it provides satisfactory results overall) that it applies, if not to the entire Sun, at least to the areas of the field open to the interplanetary medium.

4.1 Alfvén frozen field theorem

In this section, we demonstrate Alfvén's "frozen field" theorem, which describes the conservation of magnetic connections in a fluid with infinite electrical conductivity. This theorem follows from Maxwell-Faraday's equation,

$$\frac{\partial \mathbf{B}}{\partial t} = -\nabla \times \mathbf{E} \tag{59}$$

to which we add the assumption of infinite conductivity of the medium, and therefore Ohm's law of the form $\mathbf{E} = -\mathbf{u} \times \mathbf{B}$, to obtain

$$\frac{\partial \mathbf{B}}{\partial t} = \nabla \times (\mathbf{u} \times \mathbf{B}) \tag{60}$$

Alfvén's freezing theorem follows directly from this last equation, of which it is a geometric reformulation.

Consider a small element $\boldsymbol{\delta\ell}(t)$ advected by the velocity field $\mathbf{u}$ of the plasma. Let us examine how the vector product $\boldsymbol{\delta\ell} \times \mathbf{B}$ evolves over time :

$$\frac{d}{dt}(\boldsymbol{\delta\ell} \times \mathbf{B}) = \frac{d\boldsymbol{\delta\ell}}{dt} \times \mathbf{B} + \boldsymbol{\delta\ell} \times \frac{d\mathbf{B}}{dt} \tag{61}$$

The evolution of the element $\boldsymbol{\delta\ell}$ is given, if we assume $\boldsymbol{\delta\ell}$ is sufficiently small to be able to expand to first order $\mathbf{u}(\mathbf{r} + \boldsymbol{\delta\ell}) = \mathbf{u}(\mathbf{r}) + (\boldsymbol{\delta\ell} \cdot \nabla)\mathbf{u}$, by [1] :

$$\frac{d\boldsymbol{\delta\ell}}{dt} = (\boldsymbol{\delta\ell} \cdot \nabla)\mathbf{u} \tag{62}$$

while that of the magnetic field is, according to eq.(60)

$$\frac{d\mathbf{B}}{dt} = \frac{\partial \mathbf{B}}{\partial t} + (\mathbf{u} \cdot \nabla)\mathbf{B} = \nabla \times (\mathbf{u} \times \mathbf{B}) + (\mathbf{u} \cdot \nabla)\mathbf{B} \tag{63}$$

which can be reformulated, using the expression for the curl of a vector product, as

$$\frac{d\mathbf{B}}{dt} = -(\nabla \cdot \mathbf{u})\mathbf{B} + (\mathbf{B} \cdot \nabla)\mathbf{u} \tag{64}$$

where we have used Maxwell's equation $\nabla \cdot \mathbf{B} = 0$. Using these expressions, we can rewrite eq.(61) as

$$\frac{d}{dt}(\boldsymbol{\delta\ell} \times \mathbf{B}) = -\mathbf{B} \times (\boldsymbol{\delta\ell} \cdot \nabla)\mathbf{u} - (\nabla \mathbf{u})\boldsymbol{\delta\ell} \times \mathbf{B} + \boldsymbol{\delta\ell} \times (\mathbf{B} \cdot \nabla)\mathbf{u}. \tag{65}$$

However, if $\mathbf{B}$ and $\boldsymbol{\delta\ell}$ are collinear, we obviously have

$$\mathbf{B} \times (\boldsymbol{\delta\ell} \cdot \nabla)\mathbf{u} = \boldsymbol{\delta\ell} \times (\mathbf{B} \cdot \nabla)\mathbf{u} \quad \text{and} \quad \boldsymbol{\delta\ell} \times \mathbf{B} = 0. \tag{66}$$

Eq.(65) therefore shows that if $\mathbf{B}$ and $\boldsymbol{\delta\ell}$ are collinear at a given moment, they remain so at all subsequent moments (and were so at all previous moments...). In other words, an element $\boldsymbol{\delta\ell}$ describing a magnetic field line will still describe the same magnetic field line after advection by the plasma velocity field.

This result, which states the conservation of magnetic connections (i.e. the fact that two points connected by a magnetic field line at a given moment will remain so at all subsequent moments), constitutes a very strong constraint, which is lifted by taking into account a non-zero resistivity in Ohm's law (eq.60). The "unchanging" field lines of ideal MHD can then "reconnect". This is a subject that we will not address here.

1. because by definition of $\boldsymbol{\delta\ell}$ as an element advected by the velocity field, we have $d\boldsymbol{\delta\ell}/dt = \mathbf{u}(\mathbf{r} + \boldsymbol{\delta\ell}) - \mathbf{u}(\mathbf{r})$ – draw a diagram if necessary.

4.2 Parker's spiral

Here we are interested in how the conservation of magnetic connections, whose origin we have just seen, implies a particular spiral structure for the interplanetary magnetic field.

The Sun rotates on its axis in about 25 days at its equator (the rotation period is longer, almost 40 days, at the poles), giving an angular frequency of $\omega \simeq 2.9 \times 10^{-6}$ rad.s^{-1}. If we consider the magnetic field at the surface of the Sun to be fixed, these boundary conditions are therefore, in an inertial reference frame, variable in time (with the solar rotation). It is more convenient to treat the problem without explicit dependence on t, so we place ourselves in a reference frame rotating with the Sun.

In order to simplify the calculations, we will assume that we can neglect the acceleration of the solar wind beyond a certain distance $a \gg r_c$: $u(r > a) = u_0$.

In the reference frame rotating with the Sun, the solar wind velocity lines are curved : the velocity field has an azimuthal component

$$u_\phi = -\omega(r - a)\sin\theta \tag{67}$$

where θ is the co-latitude of the point considered, where we have assumed that the component u_ϕ of the velocity field was zero up to the radius a, i.e. that the solar wind was co-rotating with the Sun up to that point.

The coordinates of a small element $d\boldsymbol{\ell} = (dr, 0, r\sin\theta d\phi)$ along a velocity field line are related by

$$u_0 r d\phi = -\omega(r - a)dr \tag{68}$$

and a velocity line with initial conditions (a, ϕ_0) therefore has the following equation in spherical coordinates :

$$r(\phi) - a\ln(r(\phi)/a) = a - \frac{u_0}{\omega}(\phi - \phi_0) \tag{69}$$

which, sufficiently far from the Sun ($r \gg a$), is the equation of an Archimedean spiral, since the logarithmic term can then be neglected.

In the reference frame considered, where the system does not depend on time, the conservation of magnetic connections requires the magnetic field lines to coincide with the velocity field lines. The interplanetary magnetic field therefore has a spiral shape, known as a Parker spiral (see fig.**??**).

We can draw conclusions from this structure of the magnetic field about the radial evolution of the components of $\mathbf{B}$. The angle between a field line (small element $d\boldsymbol{\ell}$) and

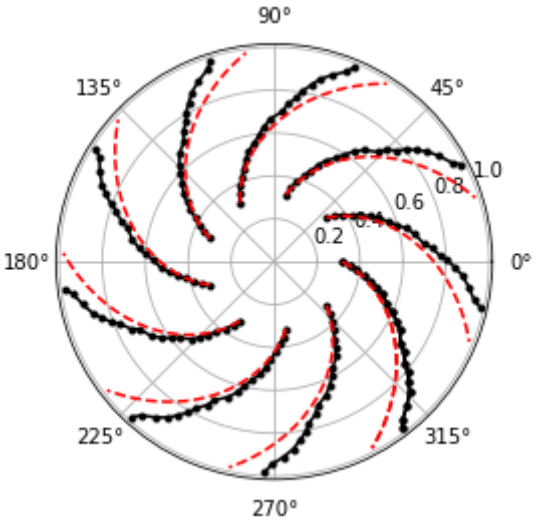

FIGURE 9 – Evolution of the direction of the interplanetary magnetic field measured by the magnetometer on board the Helios probe, for wind speeds between 250 and 300 km.s^{-1}.

the radial direction is

$$\tan\psi = \frac{B_\phi}{B_r} = \frac{r\sin\theta d\phi}{dr} = -\frac{\omega}{u_0}(r-a)\sin\theta \tag{70}$$

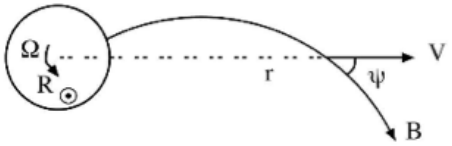

We know that the divergence of the magnetic field is zero, which, in spherical symmetry reads, for the radial component, $\partial_r(r^2 B_r) = 0$. Therefore, we have

$$B_r(r,\theta,\phi) = B(a,\theta,\phi_0)\left(\frac{a}{r}\right)^2 \tag{71}$$

from which we can deduce the azimuthal component, using (70) :

$$B_\phi(r,\theta,\phi) = -B(a,\theta,\phi_0)\frac{\omega}{u_0}(r-a)\sin\theta\left(\frac{a}{r}\right)^2 \tag{72}$$

One consequence of the spiral structure is therefore that the radial component of the field decreases as r^{-2} while (for $r \gg a$), its azimuthal component decreases as r^{-1}. The

amplitude of the magnetic field therefore follows a law of the form :

$$|B(r,\theta,\phi)| \simeq B(a,\theta,\phi_0)\left(\frac{a}{r}\right)^2\sqrt{1+\frac{\omega^2\sin^2\theta}{u_0^2}(r-a)^2} \tag{73}$$

A characteristic length of this system is therefore the distance at which the two components are equal (where the angle ψ is equal to $-\pi/4$). This distance is $r_* = u_0/\omega\sin\theta$. Close to the Sun (for $r-a \ll r_*$)), the field is essentially radial and its amplitude decreases as r^{-2}. Far from the Sun (for $r-a \gg r_*$)), the field is mainly azimuthal and its amplitude decreases as r^{-1}. The typical value of r_* in the plane of the ecliptic is 1 AU.

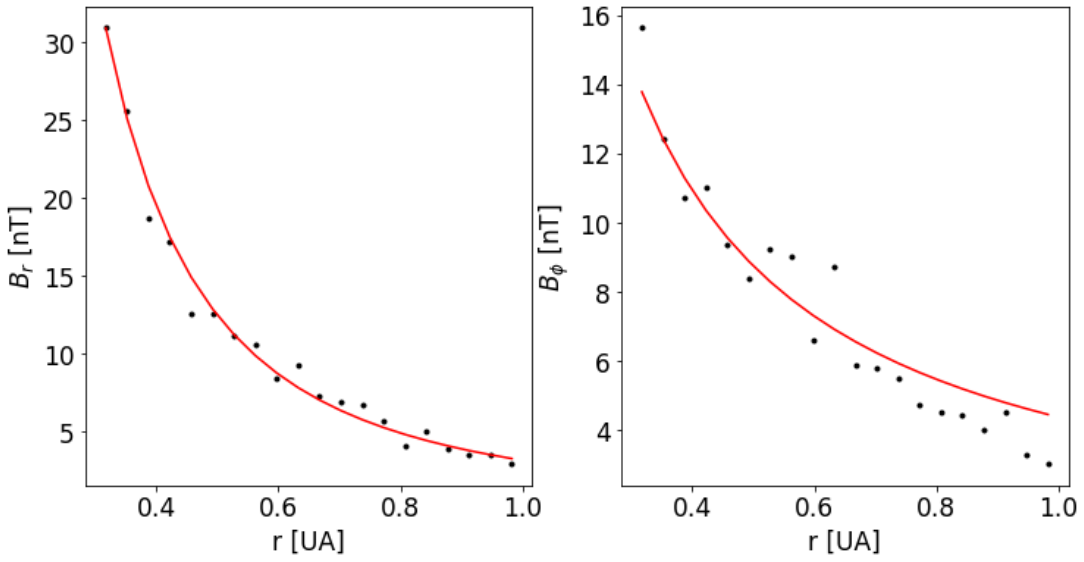

FIGURE 10 – Radial evolution of the components B_r and B_ϕ measured by the magnetometer on board the Helios probe, for wind speeds between 350 and 400 km.s^{-1}. Comparison with laws in r^{-2} and r^{-1}.

4.3 Boundary conditions, neutral layer.

$B(a,\theta,\phi)$, which appears in the previous equations, is the boundary condition imposed by the solar field, at $r = a$. Since field lines far from the Sun (we have taken $a \gg R_s$) are stretched radially by the solar wind, we can assume with good approximation that the vector B at $r = a$ is approximately radial. Since B must have zero divergence, the positive flux through the sphere of surface area a must be equal to the negative flux (in other words, there must be as many field lines entering the Sun as there are leaving it).

As a first approximation, it is natural to consider this field at the boundary as that

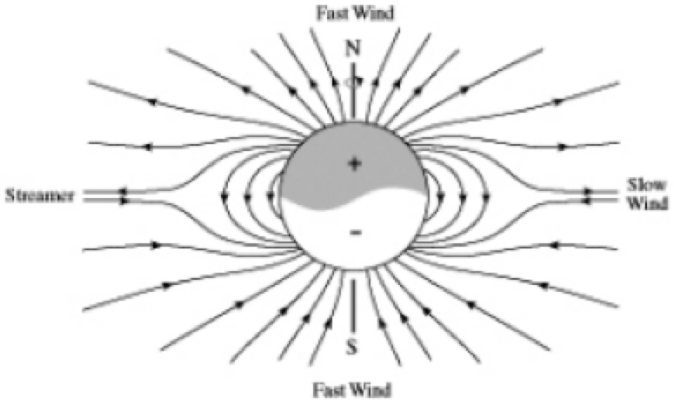

FIGURE 11 – Representation of field lines in the solar equatorial plane.

of a dipole with magnetic moment m,

$$B_r(a,\theta,\phi) = \frac{\mu_0}{4\pi}\frac{2m\cos\theta}{a^3}. \tag{74}$$

The value of B for $a = 10R_s$ is approximately 1300 nT, or 0.013 G, the gauss (1G = 10^{-4} T being often used in solar physics, like ergs and cgs units in general). It should be borne in mind that this is really an order of magnitude, which is also variable, as it depends heavily on the solar cycle (see below).

We can see from eq.(74) that the interplanetary field lines enter the Sun for $0 < \theta < \pi/2$ (northern hemisphere) and exit it for $\pi/2 < \theta < \pi$ (southern hemisphere). The magnetic field therefore changes sign around $\theta = \pi/2$ (solar magnetic equator) : this is called the neutral layer. As this layer is tilted relative to the plane of the ecliptic, an observer on Earth will see half the time (half a solar rotation period) a field pointing towards the Sun, and the other half a field pointing outwards. (cf. fig.12)

The existence of this neutral layer implies the existence of a current layer in the plasma. According to Maxwell-Ampère's equation, an azimuthal current

$$j_\phi(r) \simeq \frac{1}{\mu_0 r}\frac{\partial B_r(r)}{\partial\theta} = -\frac{m}{2\pi a}\frac{\sin\theta}{r^3}. \tag{75}$$

We used the expression for B_r and neglected the ϕ component of the magnetic field. In reality, this current is more localised in a fairly thin layer, and modelled by a non-zero current j_φ over a finite thickness in cylindrical geometry. In a simple model, we can obtain the interplanetary field by adding the dipole field to that created by the neutral layer.

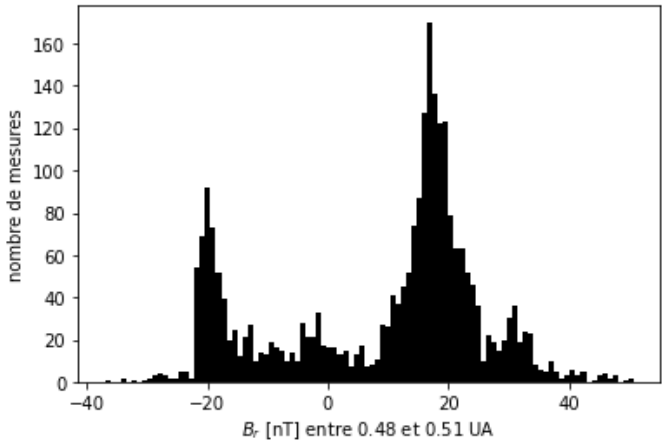

FIGURE 12 – Histogram of magnetic field values at 0.5 AU measured by the magnetometer on the Helios probe. Two peaks with opposite polarities are clearly visible for Br. In this case, the probe spent more time above (positive polarity) the neutral layer than below it during this series of measurements.

4.4 Solar cycle, slow wind and fast wind.

The solar magnetic field originates mainly from the dynamo effect in the convection zone, below the photosphere. For reasons related to the dynamics of this instability, the structure of the field varies periodically over time, with a complete cycle lasting approximately 22 years. During periods of *minimum solar activity*, approximately every 11 years, the solar magnetic field is, with good approximation, dipolar, with a magnetic moment pointing north or south (it therefore takes 22 years for the field to return to its initial configuration). During these minimum periods, the number of sunspots is low

During periods of *minimum solar activity*, approximately six years after the minimum, the magnetic field is highly multipolar. The number of sunspots is high (sunspots are regions characterised by a highly disturbed local magnetic field with high amplitude - hence the link with the multipolarity of the field on a global scale).

The structure of the magnetic field on the Sun's surface determines the boundary conditions for solar wind emission (complex effects to model that we have not taken into account in the model described in the previous section). We can intuitively understand that the effect of the magnetic field on the plasma will be to limit its mobility in the direction perpendicular to the field lines.

The wind will therefore be easily accelerated in regions where the solar B field is topologically open to the interplanetary medium, and less easily accelerated (or not accelerated at all) in regions where B is not open (B field lines connecting one point on the

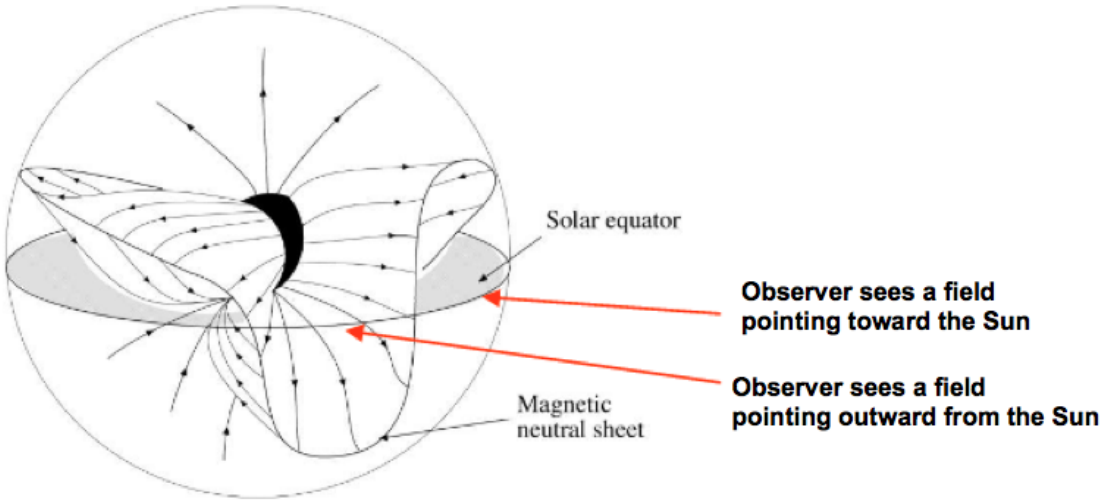

FIGURE 13 – In reality, the neutral layer is not straight but describes a curve (first-order sine) on the solar surface. This is sometimes called the "ballerina skirt" effect. The effect is greatly exaggerated in the figure.

solar surface to another).

Open regions give rise to a so-called "fast" wind (> 700 km.s^{-1}). These topologically open regions are mainly found at the Sun's poles, but also in active regions (sunspots).

In regions where the open magnetic flux is weaker, acceleration must follow more complex paths, probably via reconnection phenomena, and the wind is accelerated to lower speeds of ~ 300 km/s. This is referred to as slow wind. These regions where the slow wind emanates are mainly at the solar equator (and therefore at the neutral layer and the ecliptic plane).

It is interesting to note that slow and fast winds are characterised by quite different physical parameters (the temperature of the fast wind is higher, but its density is lower, and high-amplitude Alfvén waves are also more frequent in the fast wind and less so in the slow wind). The composition of minor species (particularly α particles) is also different in these two types of wind. In short, in many respects, these are two quite different types of environment. However, there are a number of invariants, one of which is the energy flux studied in the previous section : it depends little on the wind speed.

The large-scale structure of the solar wind is therefore strongly dependent on the solar cycle via the action of the solar B field as a boundary condition. During periods of maximum activity, this structure will be more complex than during periods of mini-

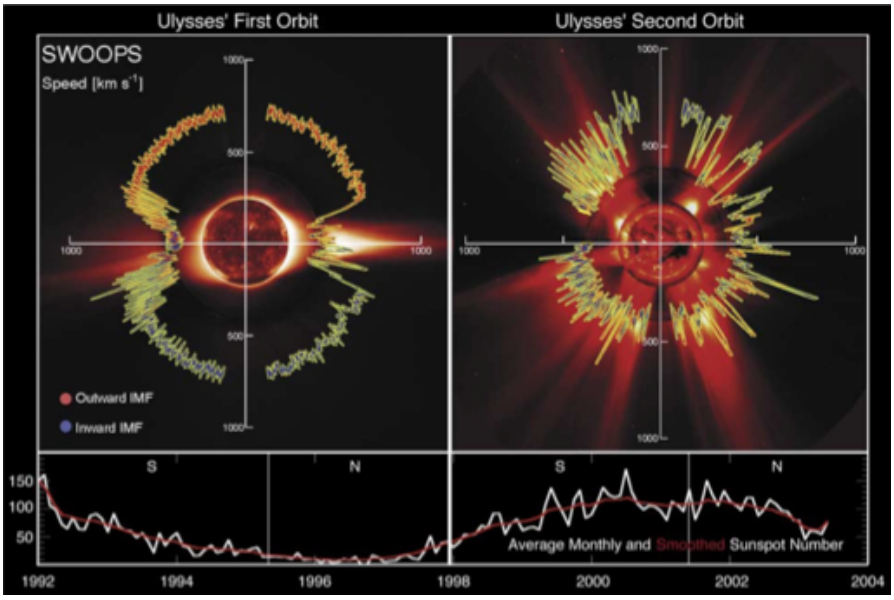

FIGURE 14 – Illustration of the solar cycle, during the Ulysses mission, showing the latitude structure of the solar wind speed and magnetic field, during periods of minimum activity (left) and maximum activity (right).

mum activity. In particular, it may exhibit numerous areas of interaction between the solar wind and the fast wind, known as "co-rotating interaction regions" (CIRs). These zones exhibit discontinuities in physical parameters (shocks), since the different magnetic configurations of fast and slow flux tubes prevent them from mixing.

4.5 Angular momentum of the solar wind, Alfvén point

So far, we have considered the solar wind velocity field to be radial. Here, we are interested in its azimuthal component u_ϕ. We will see how it is influenced by the existence of the magnetic field and its spiral structure.

The azimuthal component, in spherical coordinates, of the momentum conservation equation (2), gives

$$nm_p \frac{u_r}{r} \frac{d}{dr}(ru_\phi) = (j \times B)_\phi \tag{76}$$

where the only non-radial force is the Laplace force. This can be evaluated using Maxwell-Ampère's equation (the displacement current is neglected)

$$(j \times B)_\phi = \left(\frac{1}{\mu_0} (\nabla \times B) \times B \right)_\phi = \frac{B_r}{\mu_0 r} \frac{d}{dr}(rB_\phi) \tag{77}$$

Equation (76) can be easily integrated by multiplying both sides by r^3 and noting that $r^2 B_r = cste$ (B has zero divergence) and that $r^2 n u_r = cste$ (by conservation of particle number, or mass, see section on solar wind). We obtain

$$r u_\phi - \frac{r B_r B_\phi}{\mu_0 n m_p u_r} = \mathscr{L} \tag{78}$$

where $\mathscr{L}$ is the integration constant, which here is the angular momentum (per unit mass) of the solar wind.

In the presence of this azimuthal velocity component, the shape of Parker's spiral is slightly modified. Indeed, the velocity field in the reference frame rotating with the Sun is now $u'_\phi = u_\phi - \omega(r-a)\sin\theta$. Equation (70) of the ratio between B_ϕ and B_r is therefore modified,

$$\tan\psi = \frac{B_\phi}{B_r} = \frac{u_\phi - \omega(r-a)\sin\theta}{u_r} \tag{79}$$

This relationship allows us to eliminate B_ϕ from eq.(78), and obtain

$$u_\phi = \omega r \frac{M_A^2 \mathscr{L} r^{-2} \omega^{-1} - 1}{M_A^2 - 1} \tag{80}$$

where

$$M_A^2 = \left(\frac{u_r}{v_A}\right)^2 = \frac{\mu_0 n m_p u_r^2}{B_r^2} \tag{81}$$

is the "radial" Alfvén Mach number (here squared), i.e. the ratio between the radial wind speed and the Alfvén speed v_A calculated taking only the radial field into account. M_A is very small near the Sun (strong magnetic field and low wind speed) but is approximately $M_A \sim 10$ at 1 AU. In addition to the transonic point r_c, the solar wind passes through a second critical point : the Alfvén point, where it changes from a sub-Alfvén speed to a super-Alfvén speed.

When passing through the Alfvén point, the denominator of (80) becomes zero. Since the azimuthal velocity must still be defined at this point, this implies that the numerator also becomes zero (just as we had an indeterminate form when passing through the transonic point in Parker's model). This condition determines the value of the angular momentum per unit mass,

$$\mathscr{L} = \omega r_A^2 \tag{82}$$

which is an interesting result : if there were no magnetic field, the loss would be equal to ωR_s^2. We can see that the effect of magnetic stresses is to stiffen the motion of the plasma around the Sun, and from the point of view of angular momentum transport, it is as if the solar wind were entirely co-rotating with the Sun up to the Alfvén radius r_A.

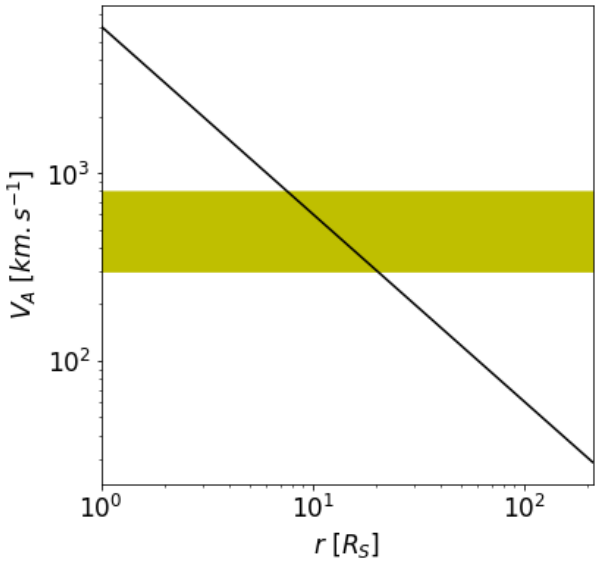

FIGURE 15 – Alfvén speed for a radial magnetic field and density model. The velocity range occupied by the solar wind is shown in yellow. We can see that the Alfvén point is roughly between 10 and 20 solar radii.

The amount $\dot{L}$ of angular momentum lost per unit time by the Sun is therefore $\dot{L} = \dot{M}\mathscr{L}$. For typical solar wind parameters, the radial Alfvén velocity varies with r as $v_A(r) = \frac{6000R_s}{r}$ km.s^{-1}. For typical wind speed values, we therefore obtain an Alfvén point at $r_A \simeq 10 - 20R_s$ (see fig.15). The amount of angular momentum lost per unit time is therefore $\dot{L} \sim 3.10^{22}$ (J.s).s^{-1}. The total angular momentum of the Sun is of the order of $L \sim 2.10^{41}$ J.s. The timescale over which the angular momentum changes significantly is therefore $\tau_L = L/\dot{L} \sim 200$ billion years. Unlike mass loss, which we have seen is not significant over the lifetime of the Sun, the variation in angular momentum due to solar wind emission represents $5 - 10\%$ of the initial momentum over its entire lifetime. Magnetised stars, in general, represent an effective channel for the dissipation of angular momentum in the universe.

Measurements also show that the tangential component u_ϕ of the velocity is much higher than the estimate (80). Tangential velocities of several tens of km.s^{-1} are observed, which is almost an order of magnitude above the theoretical prediction. This is an active area of research.

4.6 Small scales : Waves and turbulence

To be done.

4.7 Bibliography

— Interplanetary Dynamical Processes, Eugene Newman Parker, Interscience Publishers, New York, 1963
— The Angular Momentum of the Solar Wind, Weber, Edmund J. and Davis, Leverett, Jr., Astrophysical Journal, vol. 148, p.217-227, 1967

A Appendix : Fluid Equations

Here we are interested in deriving the equations of evolution for the first three centerd moments of the velocity distribution $f(\mathbf{r}, \mathbf{v}, t)$ of a population of particles. These centerd moments define the macroscopic "fluid" quantities, $n(\mathbf{r})$, $\mathbf{u}(\mathbf{r})$ and $\overline{\boldsymbol{p}}(\mathbf{r})$, namely the density, the mean velocity and the stress tensor (or pressure tensor).

The velocity distribution $f(\mathbf{r}, \mathbf{v}, t)$ is defined such that the number of particles in the phase space volume $d^3\mathbf{r}d^3\mathbf{v}$ at time t is $dN = f(\mathbf{r}, \mathbf{v}, t)d^3\mathbf{r}d^3\mathbf{v}$. Its evolution is given by an equation of the type

$$\frac{\partial f}{\partial t} + \mathbf{v} \cdot \nabla_r f + \frac{\mathbf{F}}{m} \cdot \nabla_v f = \mathscr{C}(f) \tag{83}$$

where the left-hand side can be written as df/dt describes the evolution of the distribution function along the deterministic trajectory of a particle in the force field $\mathbf{F}$, and the left-hand side is a collision operator, describing the effect of random processes on the distribution function.

We define the mean of ψ over the distribution function f as

$$\langle \psi \rangle (\mathbf{r}, t) = \frac{1}{n(\mathbf{r}, t)} \int d^3\mathbf{v} f(\mathbf{r}, \mathbf{v}, t)\psi(\mathbf{r}, \mathbf{v}, t), \tag{84}$$

where the normalisation factor is the particle density

$$n(\mathbf{r}, t) = \int d^3\mathbf{v} f(\mathbf{r}, \mathbf{v}, t). \tag{85}$$

A.1 Density

The evolution of the particle density defined above (eq.85) is obtained by integrating the kinetic equation (83) over the velocity space. We obtain

$$\frac{\partial n}{\partial t} + \nabla \cdot n\mathbf{u} = 0 \tag{86}$$

where we have used the fact that $f(v \to \pm\infty) = 0$, and where the collision operator is assumed to satisfy the property $\int d^3\mathbf{v}\mathscr{C}(f) = 0$ (which reflects the fact that no particles are created or destroyed during a collision – the operator in question does not describe chemical reactions, for example).

A.2 Velocity

We define the average velocity as $\mathbf{u} = \langle \mathbf{v} \rangle$. Its evolution is obtained by multiplying the kinetic equation (83) by $\mathbf{v}$ and integrating over the velocity. We obtain

$$\frac{\partial mn\mathbf{u}}{\partial t} + \nabla \cdot \overline{\mathbf{\Pi}} = n\mathbf{F} + n\mathbf{R} \tag{87}$$

where we have introduced a stress tensor $\overline{\overline{\mathbf{\Pi}}} = mn\langle \mathbf{vv} \rangle$ and the friction force $\mathbf{R}$ by

$$n\mathbf{R} = \int d^3\mathbf{v} m\mathbf{v}\mathscr{C}(f). \tag{88}$$

This last term describes the exchange of momentum between a population of particles described by the distribution $f(\mathbf{r}, \mathbf{v}, t)$, and external systems. This exchange is described at the macroscopic level by the operator $\mathscr{C}(f)$. The external systems may be other populations of particles, or fields, described statistically.

The tensor $\overline{\overline{\mathbf{\Pi}}}$ can be separated into a tensor of internal stresses and average stresses by introducing the random component of velocities $\mathbf{w} = \mathbf{v} - \mathbf{u}$. We then have

$$\overline{\overline{\mathbf{\Pi}}} = mn\mathbf{uu} + mn\langle \mathbf{ww} \rangle = mn\mathbf{uu} + p\overline{\overline{\boldsymbol{I}}} + \overline{\overline{\boldsymbol{\pi}}} \tag{89}$$

where the internal stresses $mn\langle \mathbf{ww} \rangle$ have been separated into an isotropic component (the pressure tensor $p\overline{\overline{\boldsymbol{I}}}$) and the actual stresses $\overline{\overline{\boldsymbol{\pi}}}$, which describe all deviations from isotropy of the distribution function (and are thus related to the viscosity of the fluid).

Using the identity $\nabla \cdot \mathbf{uu} = \mathbf{u} \cdot \nabla \mathbf{u} + (\nabla \cdot \mathbf{u})\mathbf{u}$, as well as the continuity equation (86), we can rewrite equation (87) in the more usual form

$$nm\left(\frac{\partial \mathbf{u}}{\partial t} + \mathbf{u} \cdot \nabla \mathbf{u}\right) = -\nabla p - \nabla \cdot \overline{\overline{\boldsymbol{\pi}}} + n\mathbf{F} + n\mathbf{R} \tag{90}$$

In most of this course, we will consider isotropic tensors, so $\overline{\overline{\boldsymbol{\pi}}} = 0$, and we will neglect collision effects, with $\mathbf{R} = 0$.

A.3 Energy

We obtain the equation describing energy conservation by multiplying the kinetic equation by $\frac{1}{2}mv^2$ and integrating over the velocity space. We obtain

$$\frac{\partial}{\partial t}\left(\frac{1}{2}nmu^2 + \frac{3}{2}nkT\right) + \nabla \cdot \mathbf{j}_E = n\mathbf{u} \cdot \mathbf{F} + n\mathbf{u} \cdot \mathbf{R} + nQ \tag{91}$$

where the kinetic temperature is defined by $m\mathbf{w}^2 = 3kT$. The kinetic energy flux density of the particles $\mathbf{j}_E$ is defined by $\mathbf{j}_E = n\left\langle \frac{1}{2}mv^2\mathbf{v} \right\rangle$. Q is the heat exchanged per particle and per unit time between the particle system and macroscopic external systems. This term is given by

$$nQ = \int d^3\mathbf{v} \frac{1}{2}mw^2\mathscr{C}(f), \tag{92}$$

and of course, according to the previous definitions,

$$\int d^3\mathbf{v} \frac{1}{2}mv^2\mathscr{C}(f) = nQ + n\mathbf{u} \cdot \mathbf{R}. \tag{93}$$

The energy flux density can be separated into its internal and convective parts,

$$\mathbf{j}_E = n\left\langle \frac{1}{2}mw^2\mathbf{v}\right\rangle + n\left\langle \frac{1}{2}mu^2\mathbf{v}\right\rangle + n\left\langle m(\mathbf{w}\cdot\mathbf{u})\mathbf{u}\right\rangle + n\left\langle m(\mathbf{w}\cdot\mathbf{u})\mathbf{w}\right\rangle, \tag{94}$$

and therefore

$$\mathbf{j}_E = \left(\frac{1}{2}mu^2 + \frac{3}{2}kT\right)n\mathbf{u} + (\overline{\boldsymbol{p}} + \overline{\boldsymbol{\pi}})\cdot\mathbf{u} + \mathbf{j}_{th} \tag{95}$$

where the heat flux density is defined by $\mathbf{j}_{th} = n\left\langle \frac{1}{2}mw^2\mathbf{w}\right\rangle$.

A.4 Entropy

An equation describing the evolution of the internal energy of the particle gas can be obtained by subtracting the work of forces (per unit time and volume) from equation (91). This work term is obtained by taking the scalar product of the momentum conservation equation (87) by $\mathbf{u}$. We begin by noting that for any scalar quantity ψ, the following identity is valid [2] :

$$n\frac{d\psi}{dt} \equiv n\left(\frac{\partial\psi}{\partial t} + \mathbf{u}\cdot\nabla\psi\right) = \frac{\partial}{\partial t}n\psi + \nabla\cdot\psi n\mathbf{u}. \tag{96}$$

We calculate the scalar product of equation (87) by $\mathbf{u}$. Using the previous identity, we obtain for the right-hand side

$$nm\mathbf{u}\cdot\left(\frac{\partial\mathbf{u}}{\partial t} + \mathbf{u}\cdot\nabla\mathbf{u}\right) = \frac{\partial}{\partial t}\frac{nmu^2}{2} + \nabla\cdot\frac{nmu^2}{2}\mathbf{u} \tag{97}$$

from which we obtain

$$\frac{\partial}{\partial t}\frac{nmu^2}{2} + \nabla\cdot\frac{nmu^2}{2}\mathbf{u} = \mathbf{u}\cdot(-\nabla p - \nabla\cdot\overline{\boldsymbol{\pi}} + n\mathbf{F} + n\mathbf{R}) \tag{98}$$

which expresses the conservation of macroscopic kinetic energy. Subtracting this expression from the general energy conservation equation (91), we obtain

$$\frac{\partial}{\partial t}\frac{3nkT}{2} - \nabla\cdot\frac{nmu^2}{2}\mathbf{u} + \nabla\cdot\mathbf{j}_E = \mathbf{u}\cdot(\nabla p + \nabla\cdot\overline{\boldsymbol{\pi}}) + nQ. \tag{99}$$

Finally, using equation (95) detailing the energy flux density, and simplifying this equation using identity (96) again, we finally obtain [3]

$$n\frac{d}{dt}\frac{3kT}{2} = -\nabla\cdot\mathbf{j}_{th} - (\overline{\boldsymbol{p}} + \overline{\boldsymbol{\pi}}) : \nabla\mathbf{u} + nQ, \tag{100}$$

2. the continuity equation $dn/dt = -n\nabla\cdot\mathbf{u}$ must be used to prove this.

3. where the double scalar product is defined by $\mathbf{a} : \nabla\mathbf{b} = a_{ij}\partial_{x_j}b_i$ (with summation over indices). For an isotropic tensor $\overline{\boldsymbol{p}} = p\overline{\boldsymbol{I}}$, we therefore have $\overline{\boldsymbol{p}} : \nabla\mathbf{u} = p(\nabla\cdot\mathbf{u})$.

It is interesting to note that this equation actually describes (or equivalently) the entropy production of the system. This can be seen by introducing the entropy of an ideal gas of point particles (this is the Sackur-Tetrode formula),

$$S(n,T) = k\left[\ln\left(\frac{1}{n}\left(\frac{2\pi mkT}{h^2}\right)^{3/2}\right) + \frac{5}{2}\right], \tag{101}$$

or, since the constants are not of interest here,

$$S(n,T) = k\ln\frac{T^{3/2}}{n} + cste. \tag{102}$$

The temporal evolution of entropy is therefore given by (using eq.100),

$$\frac{dS}{dt} + \frac{k}{n}\frac{dn}{dt} = -\frac{\nabla\cdot\mathbf{j}_{th}}{nT} - \frac{(\overline{\boldsymbol{p}}+\overline{\boldsymbol{\pi}}):\nabla\mathbf{u}}{nT} + \frac{Q}{T}. \tag{103}$$

Using the form $\mathbf{p} = (nkT)\overline{\boldsymbol{I}}$, we obtain the following equation :

$$\frac{dS}{dt} = -\frac{\nabla\cdot\mathbf{j}_{th}}{nT} - \frac{\overline{\boldsymbol{\pi}}:\nabla\mathbf{u}}{nT} + \frac{Q}{T}. \tag{104}$$

This equation describes the increase in entropy (per particle) of the population under consideration under the effect of three types of irreversible processes : thermal conduction, viscosity, and heat exchange with surrounding systems.

B Appendix : Maxwell stress tensor

B.1 Form of the tensor

The Lorentz force density applied to a fluid element of charge density ρ carrying a volume current $\mathbf{j}$ is given by $\mathbf{f} = \rho\mathbf{E} + \mathbf{j}\times\mathbf{B}$. This expression can be written, in general, as the divergence of a rank 2 tensor $\overline{\boldsymbol{\sigma}}_M$ that depends only on the fields $\mathbf{E}$ and $\mathbf{B}$, called the Maxwell stress tensor. The use of this form can be very practical in plasma physics, since it allows us to give a particularly compact form to the momentum conservation equation (87), as we shall see. Here we seek the form of the tensor $\overline{\boldsymbol{\sigma}}_M$.

We start from the expression for the volumetric Lorentz force, in which we express the terms ρ and $\mathbf{j}$ as functions of the fields using Maxwell-Gauss and Maxwell-Ampère equations :

$$\mathbf{f} = \epsilon_0\left(\nabla\cdot\mathbf{E}\right)\mathbf{E} + \frac{1}{\mu_0}\left(\nabla\times\mathbf{B}\right)\times\mathbf{B} - \epsilon_0\frac{\partial\mathbf{E}}{\partial t}\times\mathbf{B} \tag{105}$$

We will try to "symmetrise" this expression, i.e. give it a form in which the vectors $\mathbf{E}$ and $\mathbf{B}$ appear in terms of similar form. To do this, we begin by noting that

$$\frac{\partial\mathbf{E}}{\partial t}\times\mathbf{B} = \frac{\partial}{\partial t}\left(\mathbf{E}\times\mathbf{B}\right) - \mathbf{E}\times\frac{\partial\mathbf{B}}{\partial t} = \mu_0\frac{\partial\mathbf{S}}{\partial t} + \mathbf{E}\times\left(\nabla\times\mathbf{E}\right) \tag{106}$$

where we have introduced the Poynting vector $\mathbf{S} = \mathbf{E} \times \mathbf{B}/\mu_0$. Using this expression, we see that the Lorentz force density takes the following form

$$\mathbf{f} = \epsilon_0 \left((\nabla \cdot \mathbf{E}) \, \mathbf{E} + (\nabla \times \mathbf{E}) \times \mathbf{E} \right) + \frac{1}{\mu_0} \left((\nabla \cdot \mathbf{B}) \, \mathbf{B} + (\nabla \times \mathbf{B}) \times \mathbf{B} \right) - \frac{1}{c^2} \frac{\partial \mathbf{S}}{\partial t} \tag{107}$$

where we have added the term in div $\mathbf{B}$ (obviously equal to zero) to emphasise the symmetry of the expression in $\mathbf{E}$ and $\mathbf{B}$. We use the following vector identity

$$(\nabla \times \mathbf{A}) \times \mathbf{A} = (\mathbf{A} \cdot \nabla) \, \mathbf{A} - \nabla \left(\frac{\mathbf{A}^2}{2} \right) \tag{108}$$

to obtain the expression

$$\begin{aligned} \mathbf{f} = \epsilon_0 \left((\nabla \cdot \mathbf{E}) \, \mathbf{E} + (\mathbf{E} \cdot \nabla) \, \mathbf{E} \right) + \frac{1}{\mu_0} \left((\nabla \cdot \mathbf{B}) \, \mathbf{B} + (\mathbf{B} \cdot \nabla) \, \mathbf{B} \right) \\ - \frac{1}{c^2} \frac{\partial \mathbf{S}}{\partial t} - \nabla \left(\frac{\epsilon_0 \mathbf{E}^2}{2} + \frac{\mathbf{B}^2}{2\mu_0} \right). \end{aligned} \tag{109}$$

Finally, the formula for the divergence of a tensor $\nabla \cdot \mathbf{AA} = (\nabla \cdot \mathbf{A}) \, \mathbf{A} + (\mathbf{A} \cdot \nabla) \, \mathbf{A}$ allows us to express the force density in a relatively compact form :

$$\mathbf{f} = \nabla \cdot \boldsymbol{\sigma}_M - \frac{1}{c^2} \frac{\partial \mathbf{S}}{\partial t} \tag{110}$$

where Maxwell's stress tensor has the following expression :

$$\boldsymbol{\sigma}_M = \epsilon_0 \mathbf{EE} + \frac{\mathbf{BB}}{\mu_0} - \left(\frac{\epsilon_0 \mathbf{E}^2}{2} + \frac{\mathbf{B}^2}{2\mu_0} \right) \overline{\boldsymbol{I}} \tag{111}$$

The diagonal part of this tensor characterises the electromagnetic pressure, which acts isotropically and is expressed as

$$p_{em} = \frac{\epsilon_0 \mathbf{E}^2}{2} + \frac{\mathbf{B}^2}{2\mu_0} \tag{112}$$

The non-diagonal terms are the electromagnetic stresses themselves (we also refer to electromagnetic stresses to describe the effects of these terms).

B.2 Equation of the dynamics of a magnetised plasma

We consider a magnetised plasma in the limit of "massless" electrons $m_e \to 0$. The sum of the equations of dynamics (87) for the electron and ion populations immediately gives

$$\frac{\partial mn\mathbf{u}}{\partial t} + \nabla \cdot \overline{\boldsymbol{\Pi}} = \rho \mathbf{E} + \mathbf{j} \times \mathbf{B} \tag{113}$$

where m and $\mathbf{u}$ refer to the proton population, the "total" constraints are $\overline{\mathbf{\Pi}} = \overline{\mathbf{\Pi}}_{\boldsymbol{e}} + \overline{\mathbf{\Pi}}_{\boldsymbol{p}}$ and where we have neglected the effects of viscosity and any force other than the Lorentz force. Using the results from the previous section, we can rewrite this equation as

$$\frac{\partial}{\partial t}\left(nm\mathbf{u} + \frac{\mathbf{S}}{c^2}\right) + \nabla \cdot \left(\overline{\mathbf{\Pi}} - \overline{\boldsymbol{\sigma}}_{\boldsymbol{M}}\right) = 0 \tag{114}$$

which describes the conservation of momentum of the system consisting of particles and the electromagnetic field. It can be noted that Maxwell's constraints appear in this equation as a "negative pressure" term.

In steady state, which is useful in a large number of applications, the plasma dynamics equation is therefore reduced to a very simple equation describing the compensation at every point of the particle and field constraint terms

$$\nabla \cdot \left(\overline{\mathbf{\Pi}} - \overline{\boldsymbol{\sigma}}_{\boldsymbol{M}}\right) = 0. \tag{115}$$

To conclude this section, it should be noted that in a non-relativistic and quasi-neutral plasma, the electric energy density is always much lower than the magnetic energy density. Indeed, in this case, $\mathbf{E} \sim \mathbf{U} \times \mathbf{B}$, where $\mathbf{U}$ is the typical fluid velocity of the plasma. We therefore have

$$\frac{\epsilon_0 E^2}{B^2/\mu_0} \sim \frac{U^2}{c^2} \ll 1 \tag{116}$$

The stress tensor is therefore reduced, for the vast majority of plasma applications, to its magnetic component, $\overline{\boldsymbol{\sigma}}_M = \left(\mathbf{BB} - B^2\overline{\boldsymbol{I}}/2\right)/\mu_0$. If we consider a scalar pressure $p = p_e + p_p$ for the plasma (i.e. we neglect the non-diagonal internal stresses $\overline{\boldsymbol{\pi}}$), we have $\overline{\mathbf{\Pi}} = nm\mathbf{uu} + p\overline{\boldsymbol{I}}$ and we obtain directly from (115) the description of the dynamics

$$\nabla \cdot \left(nm\mathbf{uu} - \frac{\mathbf{BB}}{\mu_0} + \left(p + \frac{\mathbf{B}^2}{2\mu_0}\right)\overline{\boldsymbol{I}}\right) = 0. \tag{117}$$

This is a very useful conservation equation for describing the state of a magnetohydrodynamic system in steady state.

B.3 Angular momentum of the solar wind

In this section, we repeat the calculation performed in section 4.5 using the tensor relation obtained in the previous question. We consider that the vector fields only have components along $\mathbf{e}_r$ and $\mathbf{e}_\phi$, and that they are only a function of the distance r from the center of the sun (and the reference frame). Under these conditions, the expression for the tensor divergence in spherical coordinates is

$$\nabla \cdot \overline{\boldsymbol{T}} = \left(\frac{\partial T_{rr}}{\partial r} + \frac{2T_{rr} - T_{\phi\phi}}{r}\right)\mathbf{e}_r + \left(\frac{\partial T_{r\phi}}{\partial r} + \frac{3T_{r\phi}}{r}\right)\mathbf{e}_\phi \tag{118}$$

The cancellation of the azimuthal component of equation (117) imposes

$$\frac{1}{r^3}\frac{d}{dr}\left(r^3 n m u_r u_\phi - \frac{r^3 B_r B_\phi}{\mu_0}\right) = 0. \tag{119}$$

Using the conservation of mass flux $r^2 n m u_r = cste$, we directly obtain the result

$$\frac{d}{dr}\left(r u_\phi - \frac{r B_r B_\phi}{n m u_r \mu_0}\right) = 0. \tag{120}$$

Exercise (not too difficult with this formalism) : show, for example, by considering a pressure tensor of the form $\overline{\boldsymbol{p}} = p_\parallel \mathbf{bb} + p_\perp(\overline{\boldsymbol{I}} - \mathbf{bb})$ (where $\mathbf{b}$ is the unit vector along the magnetic field) that an anisotropy of the particle distribution functions contributes to the angular momentum per unit mass of the solar wind.